THE UNIVERSITY OF OKLAHOMA

GRADUATE COLLEGE

PASSIVE MICROWAVE MEASUREMENT OF WATERSHED RUNOFF CAPABILITY

A DISSERTATION

SUBMITTED TO THE GRADUATE FACULTY

in partial fulfuillment of the requirements for the

degree of

DOCTOR OF ENGINEERING

BY

BRUCE JOHN BLANCHARD

Norman, Oklahoma

1974

PASSIVE MICROWAVE MEASUREMENT OF WATERSHED RUNOFF CAPABILITY

APPROVED BY

ACKNOWLEDGMENT

The author wishes to express his sincere gratitude to the many individuals and organizations who assisted in accomplishing the study for preparation of this thesis. Appreciation is extended to Dr. J. F. Harp for his acceptance of a pragmatic approach toward solution of watershed runoff problems and his encouragement throughout the program of study. Thanks are also extended to the other members of the Doctoral Committee for their interest and aid in this project.

Data used in this study were supplied by the National Aeronautics and Space Administration - Johnston Space Center and the Agricultural Research Service of USDA. The data was gathered in a cooperative investigation with Dr. T. Schmugge, Goddard Space Center and Dr. J. W. Rouse, Jr., Texas A&M University - Remote Sensing Center. The discussion and technical advice from these two cooperators and Mr. Richard Matthews, Johnson Space Center, has been greatly appreciated.

Numerous men in the Program Planning Office, Flight Operations, Data Management and Lockheed support groups all from the Johnson Space Center have contributed exceptional effort to provide the best techniques available for collection and preparation of data for this study. Each who has contributed deserves sincere thanks.

TABLE OF CONTENTS

LIST OF TABLES

LIST OF FIGURES

Figure Page

ABSTRACT

Remote sensing is potentially an economical means of obtaining the areally distributed runoff potential of a watershed. This assumes that the runoff potential can be accurately predicted as a function of watershed surface characteristics.

The average microwave temperature of the watershed surface as detected by an airborne Passive Microwave Imaging Scanner (PMIS) was compared to the average annual watershed runoff and the measured Soil Conservation (SCS) watershed storm runoff coefficient (CN). Previous laboratory work suggests that microwave response to the watershed surface is influenced by some of the same surface characteristics that affect runoff, i.e., soil moisture, surface roughness, vegetative cover and soil texture.

In order to field test and develop relations between runoff potential and microwave response, several highly instrumented watersheds of approximately 1.5-17 km^2 were scanned under wet and dry soil conditions in April and June 1973. The polarized (horizontal and vertical) scans at 2.8 cm wavelength provided the data base from which other values were calculated. Lower SCS runoff coefficients appear to be correlated to the cross polarized response under dry watershed conditions late in the growing season and the difference in horizontal polarized response between wet conditions early in the growing season and dry conditions late in the growing season. The best relationship with runoff

coefficients was with horizontally polarized PMIS temperatures from the near-dormant early growing season flight. Apparent relations were also observed between the average annual runoff and microwave response, however, they are not well defined.

To apply the results, further verification of the relationships is needed. Moreover, a more rapid, low cost data processing system is needed to make routine application of this technique practical.

PASSIVE MICROWAVE MEASUREMENT OF WATERSHED RUNOFF CAPABILITY

CHAPTER I

INTRODUCTION

Hydrologists have long been concerned with identification of watershed surface characteristics and measurement of the influence of surface conditions on the rainfall-runoff relation. Early-day conservationists recognized that dense vegetative cover, porous soils, rough surfaces, and reduced slopes decrease storm runoff.

Modification and control of runoff from agricultural watersheds became more important in the development of the United States when people began moving westward across the Great Plains and into the semi-arid regions of North America. The establishment of the Department of Interior stimulated interest in conservation in general, and thus, in the effects of surface conditions on runoff. The occurrence of the dust bowl conditions of the thirties in the Southern Plains dramatically increased the government's participation in the application of conservation practices and led to the development of the present-day Soil Conservation Service. Legislated authority of these government agencies tend to restrict the interest of each to different size watersheds. Originally, the Department of Interior was interested in watersheds of

relatively large drainage area and the United States Geological Survey therefore collected data on large watersheds. At the same time, the U. S. Department of Agriculture, Soil Conservation Service, concerned itself with so-called unit source areas seldom larger than 100 acres in drainage area.

In recent years, both agencies have found need for runoff prediction schemes and basic data for intermediate size drainage areas ranging from 1.3 square kilometers to as much as 518 square kilometers. Other newer government agencies, Housing and Urban Development, Environmental Protection Agency, as well as county governments, state governments, consulting engineers, and private corporations have also been confronted with the need for runoff prediction on intermediate size watersheds. Very few of these watersheds have adequate records to develop a reliable historical rainfall-runoff relation. As yet, new concepts in complex mathematical modeling have not been developed to a point where the models can be readily applied to an ungaged watershed. The less complex models available are empirical in nature, using three or four measurable watershed characteristics (Chow, 1964).

The coefficients of these models are generally related to the ability of the watershed surface to store or detain part of the storm rainfall. Part of the rainfall that infiltrates the surface may ultimately reach the stream as low flow. Storm runoff equations do not apply to this part of runoff unless the subsurface return to streamflow is rapid. Return flow from groundwater storage and interflow through the soil are associated with soil permeability.

A watershed with heavy vegetation, permeable soils, rough surfaces, and low slopes will tend to produce less surface runoff. The Soil

Conservation Service has established a series of tables relating soils and vegetative cover to a coefficient used in their storm runoff equation. There is considerable question as to the validity of techniques used to estimate these values. Application of the technique to each soil cover unit in a drainage area and integrating the tabulated results is also a tedious time-consuming effort.

The recent development of remote sensing techniques may offer faster, more independent evaluation of these near-surface characteristics. Some remote sensing techniques, notably photo interpretation and photo stereo mapping of topography have been used for a number of years in a qualitative sense for watershed evaluation. In the past decade, color and color infrared photography have become available in some areas. Color photography has aided in land use and soils classification, but at present, is not used for watershed studies. Photographic data are generally difficult to convert to quantitative form and hydrologists find it difficult to get meaningful numerical data from photographs for use in mathematical models.

Electrical optical sensors have been successfully used to obtain much the same information as would be collected on film. These devices avoid the problems of film quality and lack of stability in film developing. In the electrical optical scanner, reflectance is monitored by a photoelectric cell for each wavelength band and the output analog voltage is then converted to digital values. Such sensors are calibrated against a known source, thus the digital values may be more repeatable than film data.

Photographic data are restricted to wavelengths in the visible and near infrared region of the spectrum, however, electrical optical sensors

can be built to be sensitive to wavelengths in visible, near infrared and far infrared or "thermal" regions. Except for transparent targets, either system can only sense the surface of the first object in the line of sight, thus if they are used to detect conditions to some depth in a watershed surface, the detection is by inference only. Longer wavelengths are necessary to penetrate a material or sense conditions at a given depth.

Passive microwave systems have been developed in the past decade with antennas capable of receiving low energy natural emission in wavelengths ranging from a few tenths of a centimeter up to 20 centimeters. The advent of longer wavelength sensors may enable hydrologists to quantify a composite of the watershed surface conditions.

CHAPTER II

STATEMENT OF THE PROBLEM

The objective of this study is to determine if any relation is apparent between energy received at the antenna of an airborne passive microwave system and either annual watershed yield or watershed storm runoff potential. It is a study of the feasibility for remotely measuring a composite of the near-surface watershed characteristics that influence the disposition of rainfall at the watershed surface.

The study is confined to the use of an aircraft-mounted system known as the Passive Microwave Imaging System (PMIS). The PMIS is an X band (10.69 Ghz frequency or 2.8 cm wavelength) scanning radiometer built for and operated by the National Aeronautics and Space Administration (NASA). Since this system has not previously been used for studies over watershed drainage areas, data processing techniques were developed to reduce the microwave data to a usable form.

A review of literature pertaining to past experiments with passive microwave equipment related to soils or terrain cover reveals that microwave response is influenced by the same surface conditions that would influence rainfall-runoff relations. No attempt has been made to measure the influence of any one watershed surface characteristic on rainfall-runoff relations. Instead, this study will consider the combined watershed surface characteristics, surface soils, vegetation,

surface roughness, and soil moisture storage capacity as a single variable that may be measured by averaging microwave temperatures over a watershed.

CHAPTER III

REVIEW OF PASSIVE MICROWAVE EXPERIMENTS RELATED TO HYDROLOGY

In any discussion of passive microwave systems, one must recognize the distinction between passive and active, or radar, microwave systems. Passive microwave implies that only the natural emission of energy without input from any artificial source is being observed. The passive microwave system measures only the emission of radiant energy from a surface created by atomic and molecular oscillations in the observed material. Active or radar microwave systems on the other hand generate a signal, direct it to the surface and receive the return signal. The difference in signals sent and received is dependent on the scattering of energy at the target. Natural emission of energy measured by passive microwave systems is thus part of the noise received in the active system. The microwave region is defined as that portion of the spectrum (Fig. 1) with wavelengths 1 millimeter to .8 meter in length. However, design criteria for airborne antenna has restricted development of the airborne passive microwave systems to wavelengths less than 25 centimeters.

There are two characteristics of the portion of the spectrum with wavelengths from 1 centimeter to 25 centimeters that suggest that wavelengths in this region may be useful for hydrologic application. First, and most important, is the fact that these wavelengths, in a sense, can penetrate the surface of material. Penetration of passive microwaves

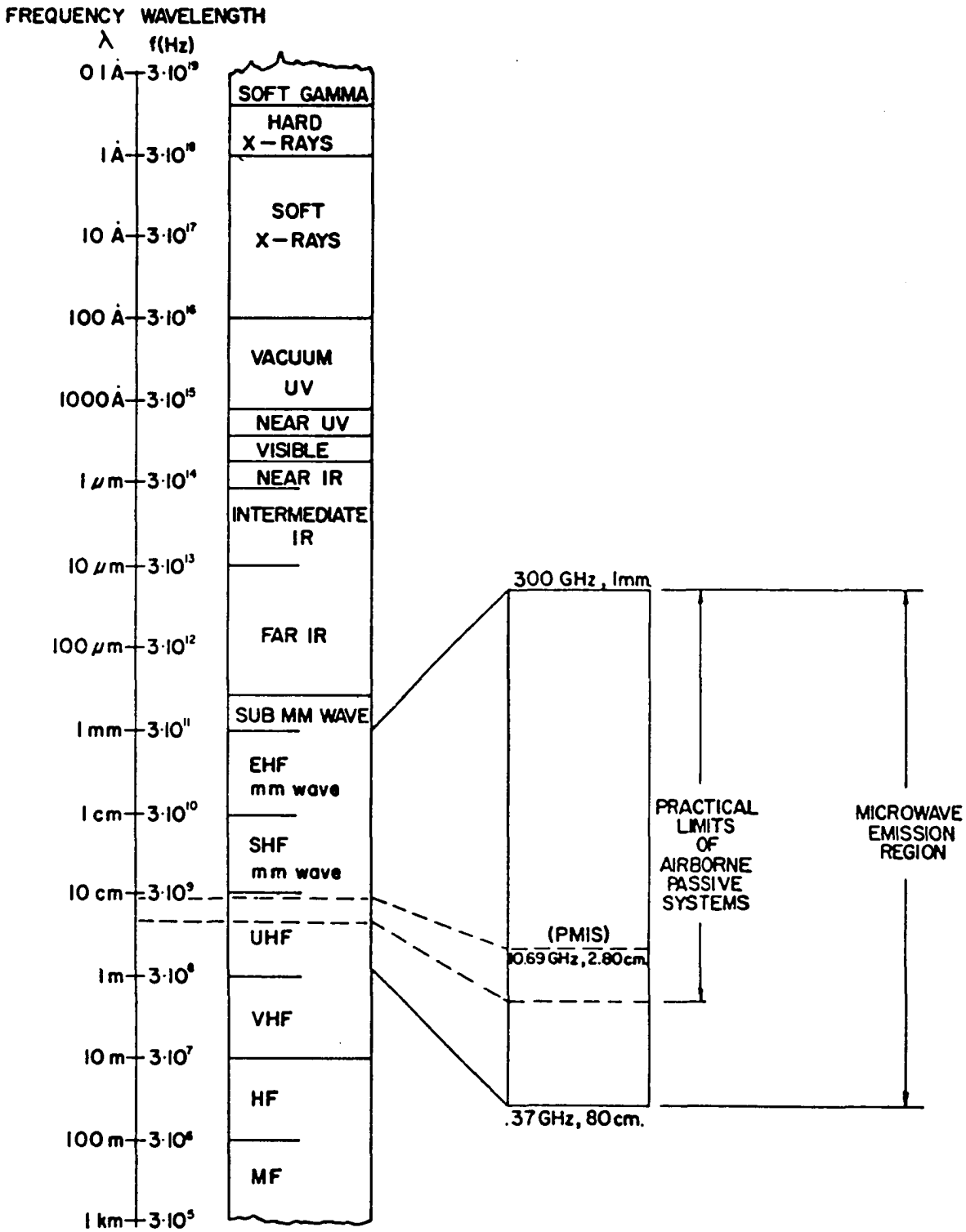

Figure 1. Spectrum

might be described more adequately as the depth from which emitted energy may originate and still escape through the air surface interface. The depth increases with longer wavelengths and is greater for sandy porous soils than for clay soils. Selection of proper wavelengths could allow hydrologists to examine conditions at a given depth below the soil surface.

Reflective aluminum plates covered by soil have been used (Conway, 1966) to determine depths that a radiometer can detect changes under a dry soil. For dry clay, the depth of penetration was approximately 15 cm, while dry sand could be penetrated to nearly 60 cm. Similar tests using an active microwave system (Lundein, 1971) have shown comparable results on a greater range of materials. These tests also showed that in dry material, longer wavelengths could penetrate to greater depths than short wavelengths. Conway does not mention how samples of soil were prepared, however Lundein compacted his samples with at least three different pressures and found no significant change in response for changes in compaction pressures of ±25 percent. A study (Blinn, 1972) in which a reflector was covered with dry fine sand at increasing depths showed that response from the reflector was influenced by interference related to particle size. Results of these experiments would indicate that penetration in natural soil profiles is a dynamic phenomenon and will be difficult to quantify at a point in the field, however the ability to sense soil conditions at some depth below the surface does exist.

The second characteristic of the spectrum that may be useful in hydrologic application is the possibility that energy radiated in this region is relatively free from influence of atmospheric conditions

(see Fig. 2). In many areas of the spectrum, atmospheric attenuation can seriously hamper remote sensing of the earth surface. At times it totally nullifies the results. Ordinary aerial black and white or color photography for instance, senses wavelengths short encugh that they can not penetrate clouds. When cumulus clouds are present they can be easily identified; however, if thin cirrus clouds or haze are present in the atmosphere, the subtle effect on the image may not be recognized. It is important to realize that atmospheric interference does not affect all wavelengths the same way. In some regions of the spectrum, there is no atmospheric interference.

Attenuation due to atmospheric interference in wavelengths immediately below 1.5 centimeter are severe. This led to use of shorter wavelengths, in the microwave region, to sense humidity and precipitable water. A peak attenuation or responsiveness to water vapor is found near 1.35 centimeters wavelength. Another peak for molecular oxygen is located at .5 centimeters wavelength (Hopkins, 1962). Water vapor attenuation also occurs in wavelengths less than .5 centimeters (Fig. 2), thus it is desirable to select sensors adapted to the range from 2- to 25-centimeter wavelengths when examining the earth's surface.

A simple graphic illustration (Fig. 3) can be used to show what is sensed with a passive microwave radiometer. The figure shows that the sensed information is made up of both emission from the ground surface and reflected solar radiation. This is described by the equation

$$T_a = \varepsilon T_g + (1-\varepsilon)\ T_s \qquad (1)$$

The radiometric temperature at the antenna is shown to be a function of

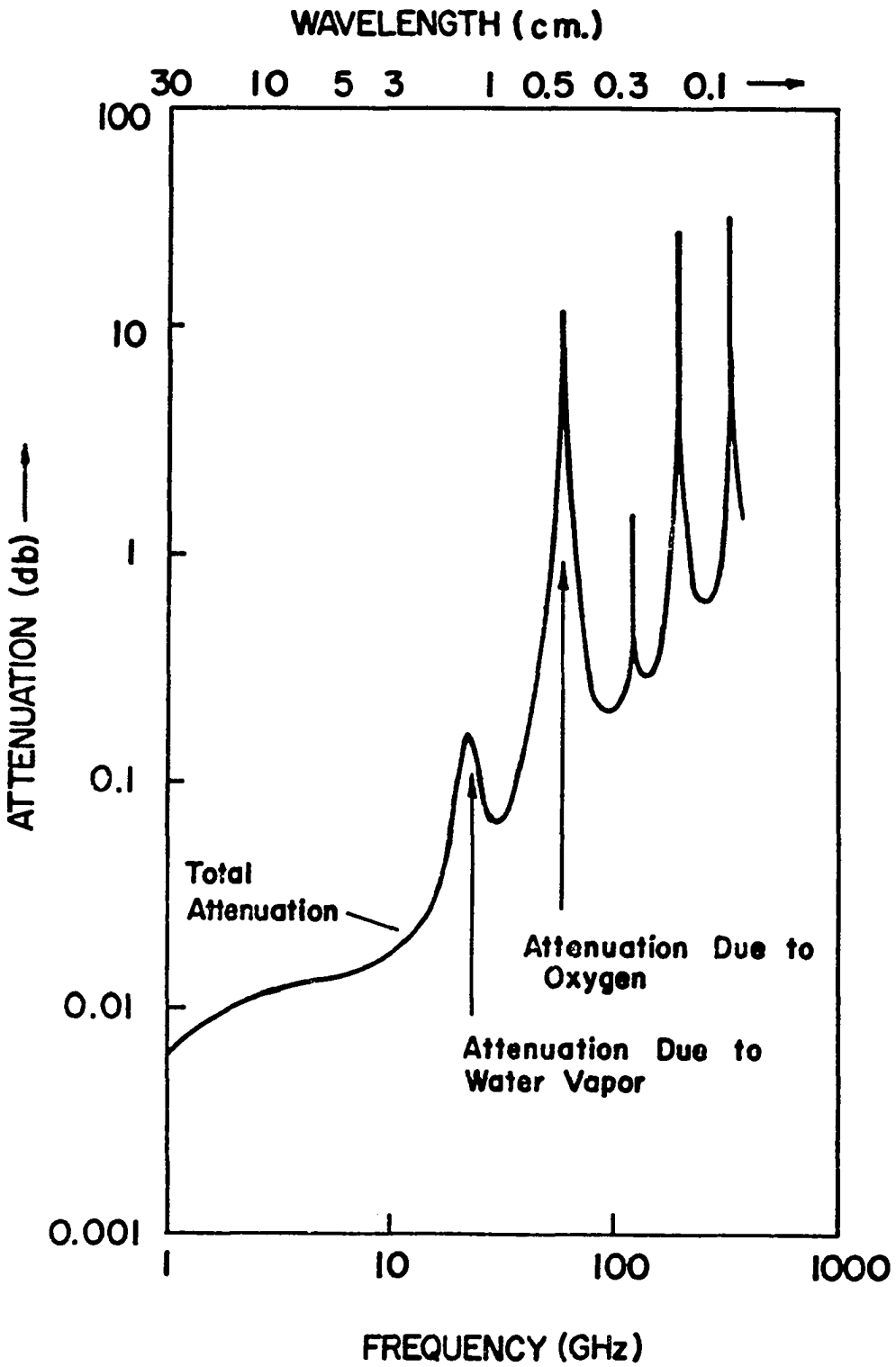

Figure 2. Atmospheric Attenuation of Microwave Energy

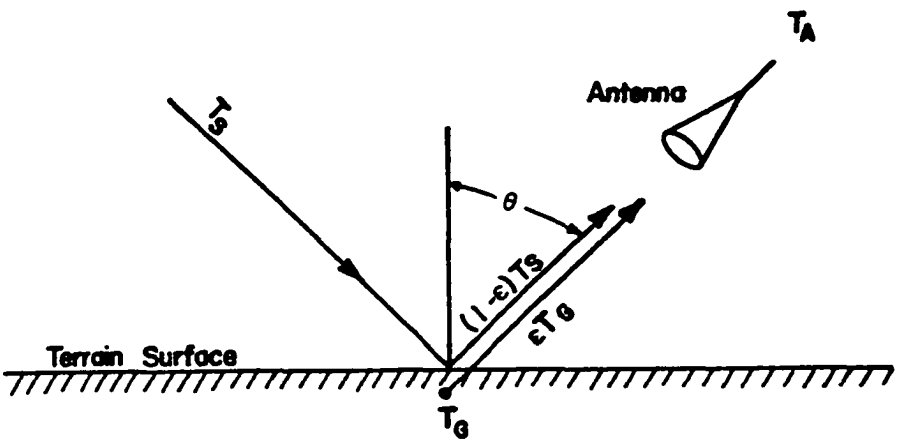

$T_A = \epsilon T + (1 - \epsilon)T_S$, $\epsilon = f\ (e' - Je'')$

where:

T_A = apparent brightness temperature (degrees Kelvin)

T_S = brightness temperature of sky (degrees Kelvin)

T_G = thermometric temperature of ground (degrees Kelvin)

ϵ = emissivity (dimensionless)

$1-\epsilon$ = reflection coefficient (dimensionless)

θ = antenna viewing angle

e' = real part of dielectric constant

e'' = imaginary part of dielectric constant

J = constant (dimensionless)

Both e' and e'' are a function of soil type and free water in the soil water mix

Figure 3. Near Surface Energy Sensed by Passive Microwave Antenna

the ground temperature, T_g; the radiometric sky temperature, T_s; and the emissivity, ε. The earth's surface receives its primary energy from the sun; consequently the ground temperature is, in turn, influenced by cloud conditions. Emissivity, ε, is large in respect to the reflectance coefficient, $(1-\varepsilon)$, and T_g is large in respect to radiometric sky temperature, T_s. The product of emissivity and ground temperature, εT_g, is therefore extremely large with respect to the reflective component $[(1-\varepsilon)\ T_s]$. Therefore, ground temperature differences produce corresponding changes in the antenna temperature. In order to avoid the local surface cooling produced by passing cloud shadows, it is desirable to acquire data in a clear weather condition. It is also necessary to acquire surface temperature measurements at the same time that radiometric temperatures are recorded in order to isolate emissivity as a function of surface conditions. Surface temperatures can be readily measured with instruments operating in the far or "thermal" infrared region of the spectrum.

Emissivity of microwave energy from terrain is influenced by the following factors: (1) Moisture present in the soil or vegetative matter on the surface, (2) roughness of the surface, (3) physical dimensions of the surface, (4) vegetative cover, and (5) the viewing angle of the antenna. The first three factors are, in a geomorphic sense, interrelated and when the surface is bare, the influence of the geology of the parent material would be present in all three characteristics. Numerous investigations of microwave emission have been directed toward evaluating the effects of one or more of these factors. Isolating each one and its effects on the microwave temperatures is expensive, therefore the amount of data available to any one investigator is limited. Little information

is available concerning passive microwave response to Factor No. 4 (vegetation). The influence of Factor No. 5 can be readily controlled by designing the radiometer with a constant viewing angle.

In recent years, many investigators have used airborne equipment for field tests because truck-mounted equipment was not available. This can lead to problems because without proper preliminary laboratory experimentation on fundamental principals, adequate control and isolation of the above factors is rarely possible.

The influence of moisture content in the surface soils on microwave emission is of major importance in application of microwave techniques in hydrology. At normal temperatures, water has an extremely high dielectric constant, 75 to 80; whereas, dry soil has a dielectric constant ranging from 3 to 5. Figure 4 from Schmugge (1974) illustrates the inverse relation between dielectric constant and emissivity and the drastic influence of soil moisture on the resulting emissivity. Characteristics such as salinity and water temperature have also been found to influence emissivity (Paris, 1969), however these have not been shown to be detectable in the studies of soil moisture or soil-water mix. The isolation and measurement of soil moisture for use in agriculture have been the driving force in the development of microwave technology. Several studies by Texas A&M University, Goddard Space Flight Center, and the U. S. Department of Agriculture, Agricultural Research Service (Jean, 1971; Kroll, 1973; Schmugge, 1974; Blanchard, 1972) have indicated that the antenna temperatures of X-band (2.8 centimeters) radiometers declined about 1.5 degrees Kelvin per 1 percent increase in soil moisture on smooth bare ground. Soil moisture measurements with L-band radiometers

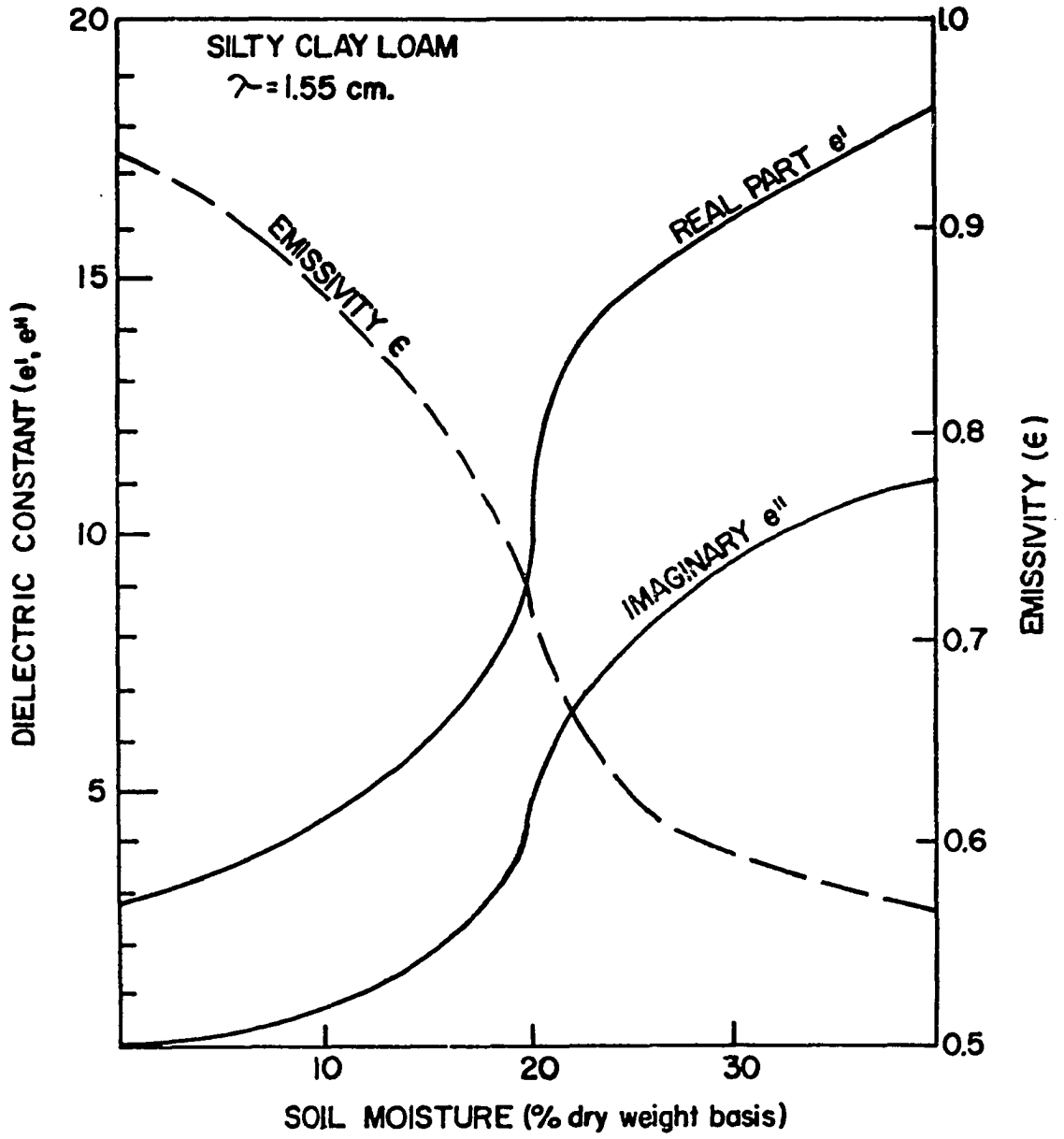

Figure 4. The Relation of Dielectric Constant to Emissivity

(20 centimeters) have shown that longer wavelengths are more sensitive to changes in soil moisture (Schmugge, 1974; Paris, 1974). Horizontally polarized temperature measurements at L band decreases about 3 degrees Kelvin for each 1 percent increase in soil moisture. The other surface characteristics influencing emissivity or antenna temperature, roughness, vegetation, and soils, are considered confusion factors that must be defined before an operational system of soil moisture monitoring with microwave equipment can be implemented.

Water, in various states of roughness, offers a unique opportunity to study influences of roughness on microwave temperatures. The uniformity of background material offered by water leaves only the roughness of waves as a variable to influence changes in emissivity when an area of uniform salinity is selected. Hollinger (1971) showed that roughness increased the signal received by the antenna. His study of three wavelengths, also showed the horizontal polarization was more sensitive to roughness than the vertical polarization. Theoretical studies (Sibley, 1973) have also indicated the effects of roughness would be significant. Since 1969 considerable effort has been directed to identifying and modeling the effects of roughness on natural terrain (Jean, 1971; Richerson, 1971; Sibley, 1973). They all found the roughness effects difficult to model mathematically, and no two investigators have settled on a uniform measure of roughness. Measures of roughness at microwave frequencies are dependent on wavelength used. A surface that is rough at 2.8 cm X-band wavelength is quite smooth in 20 cm L-band measurement. Their studies, however, have all shown that before one can adequately isolate and sense any other physical parameter of the bare soil, the

effect of the roughness must be accounted for. Blinn illustrated this point dramatically by merely raking a smooth surface of sand with a garden rake after taking radiometer temperature measurements of the soil with various amounts of soil moisture. The rake teeth were spaced approximately 2 centimeters apart. When the smooth surface was raked parallel to the horizontal polarization of the radiometer, the influence of soil moisture on the observed temperatures for wavelengths of .95 and 2.8 centimeters was essentially eliminated.

The influence of differences in soil particle size on microwave emission would appear to be very minor in view of measurements of dielectric measurements made with active and passive microwave laboratory-type equipment. Lundein (1971) found very little difference in relative dielectric constants for Oklahoma soils. When all soils in his study are grouped on a single plot, one cannot detect any difference between Eufala fine sand and Vernon clay loam. Measurements for Lundein's study were made with frequencies ranging from 1.074 to 1.499 Ghz and results indicate these soils would all have a relative dielectric constant near 3.0 at zero moisture content, thus they should all produce high emissivity and high antenna temperatures when dry.

Soil samples from the study area where this experiment was undertaken were tested for relative dielectric constants using a 9.0 Ghz frequency. All but one soil showed low dielectric properties when dry, similar to Lundein's measurements; however, some differences are evident between soils as the relative dielectric constant increases with percent moisture content. Measurements of emissivity (inverse to relative dielectric constant) were made on two sizes of sand (Malentyev, 1972) where

sand with a mean size of .20 millimeters produced an emissivity of .933 while sand with a mean size of .05 millimeters had an emissivity of .884. These values would indicate that a slightly higher antenna temperature could be expected over coarse sands. Changes in emissivity due to soil particle size can be considered quite small in comparison to changes due to free water in the soil-water mix.

Measurement of emissivity from vegetation has been limited to a very few investigations. Riegler (1966) measured standing crops of wheat and oats on the Purdue University Agronomy farm. Resulting antenna temperatures were high and indicated a relatively rough microwave surface. He was able to predict the response reasonably well using a mathematical model of roughness. Reference to these tests were made by Peake, et al. (1966) showing that the plots illustrated higher emission from wheat than from oats. The wheat contained 16 percent less moisture than the oats. They then attributed part of the difference to the crop moisture, but insufficient evidence has been accumulated at present to prove a relation exists between crop moisture and microwave temperature.

Further evidence of high emission from vegetation has been found in studies reported by Poe and Edgerton (1973). Soil moisture samples were collected in this study in vegetated fields and no evidence was found that the influence of the soil surface could be detected through the crop. Wavelengths used in these experiments were 2.2 and 6 centimeters. Malentyev reports, using a wavelength of 3.2, dry grass 15 to 20 centimeters in height produced emissivities of .935. This would result in antenna temperatures on a summer day very nearly the same as Peake and Riegler found in standing wheat with 60 percent moisture. The influence

of vegetation on microwave temperature appears to indicate nearly constant high emissivities for wavelengths shorter than 20 centimeters. Data collected at Texas A&M University (Paris, 1974) indicate that the L-band radiometer effectively penetrated a cover of both live and dead oat grass and was reasonably responsive to changes in soil moisture. It is evident that no one has devoted the necessary effort to thorougly understand changes in passive microwave temperatures throughout a growth cycle for the various types of vegetation expected in an agricultural environment. Most investigators who have studied vegetative effects on passive and active microwave temperature have expressed belief that longer wavelengths may be able to detect near-surface soil moisture conditions under vegetation.

It is evident from the past experiments that antenna temperatures are high for low soil moisture content, rough surfaces, sandy soils, and dense vegetation. All of these conditions would tend to reduce watershed runoff and if an integrated temperature for individual watershed drainage areas could be obtained, it should be related to the ability of that watershed to produce runoff. A proposal was made (Blanchard, 1972) that the unexplained anomalies in passive microwave antenna temperatures may not need to be precisely defined for calibration of watershed runoff.

To eliminate the influence of any unexplained but repeatable anomalies, it was suggested that average microwave temperatures for individual watersheds would be obtained under both saturated and dry conditions and the difference between saturated condition microwave temperatures and low moisture microwave temperatures could be used as an index of the watershed surface storage capacity. A relatively short period would be

required between wet and dry measurements to insure little change in vegetation between measurements if microwave measurements are made in the growing season, while longer time periods would be acceptable in dormant seasons.

CHAPTER IV

DESIGN OF THE EXPERIMENT AND DESCRIPTION OF EQUIPMENT

A limited knowledge of the passive microwave imaging system (PMIS) is necessary to the understanding of the design of this experiment.

Very few passive microwave imaging systems have been manufactured and flown over earth resources project areas. The PMIS is a first of its kind in that its antenna is a phased array (Louapre, 1968) with vertical and horizontal polarization channels and is electronically stepped for scanning. The antenna is located in a radome attached to the underside of the fuselage of the NP-3A NASA aircraft (Fig. 5). The electronic scanning scheme permits conical scanning, at an angle of 50 degrees from the vertical, a series of 44 beam positions across the aircraft flight path. The farthest beam positions from the nadir path is approximately 33 degrees on either side. The system is capable of recording an antenna temperature for both vertical and horizontal polarization at each of the 44 beam positions (McAllum, 1973).

A separate antenna is used for each polarization and each is scanned simultaneously at each beam position. At the end of each scan line (44 points), two hot loads are measured for calibration purposes. The sketch (Fig. 6) illustrates the configuration of the image and location of the beam positions.

The signal received at the antenna of the passive microwave radiometer is relatively weak and must be amplified considerably. The amplified

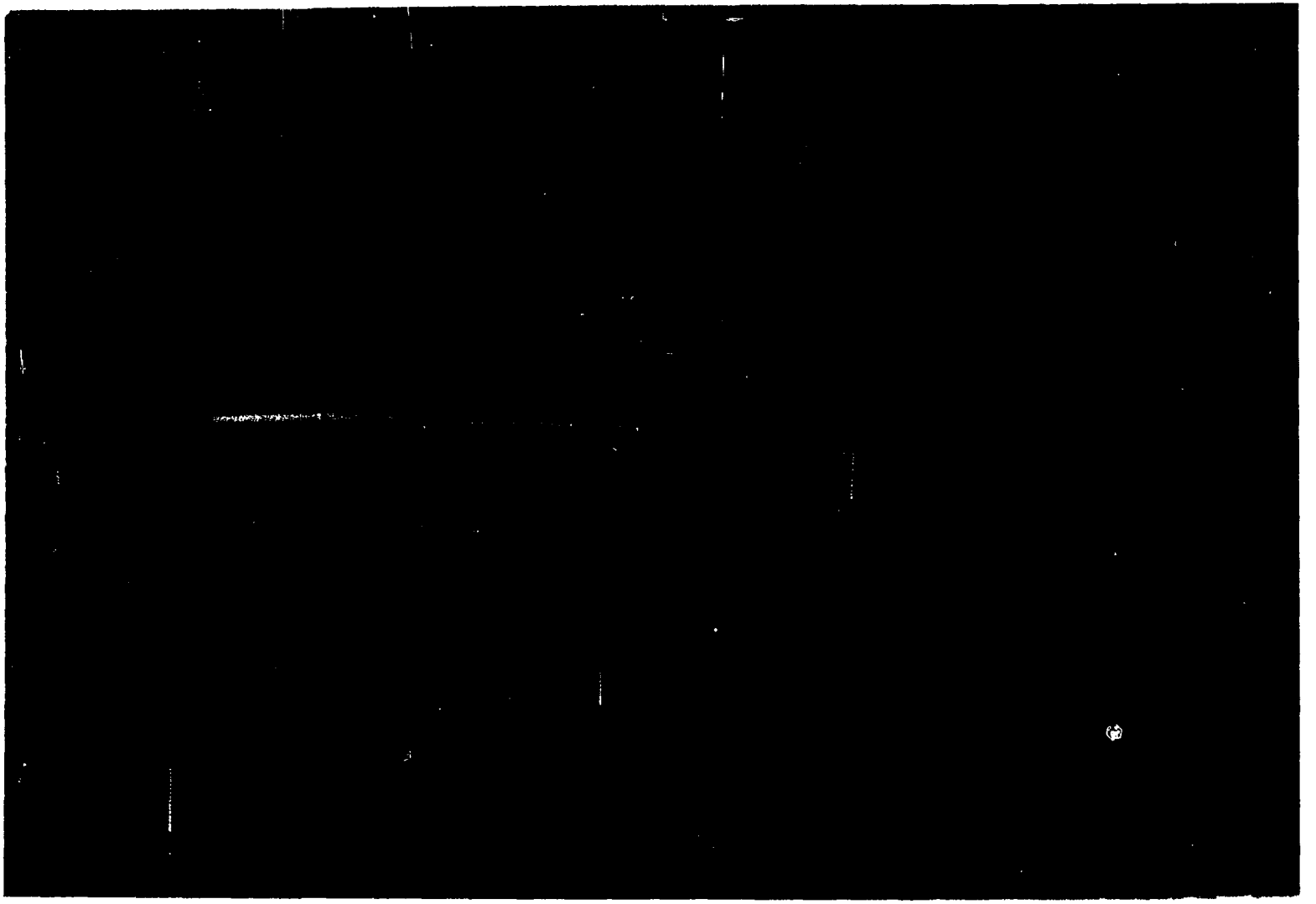

Figure 5. The NASA-P3A Aircraft with Radome

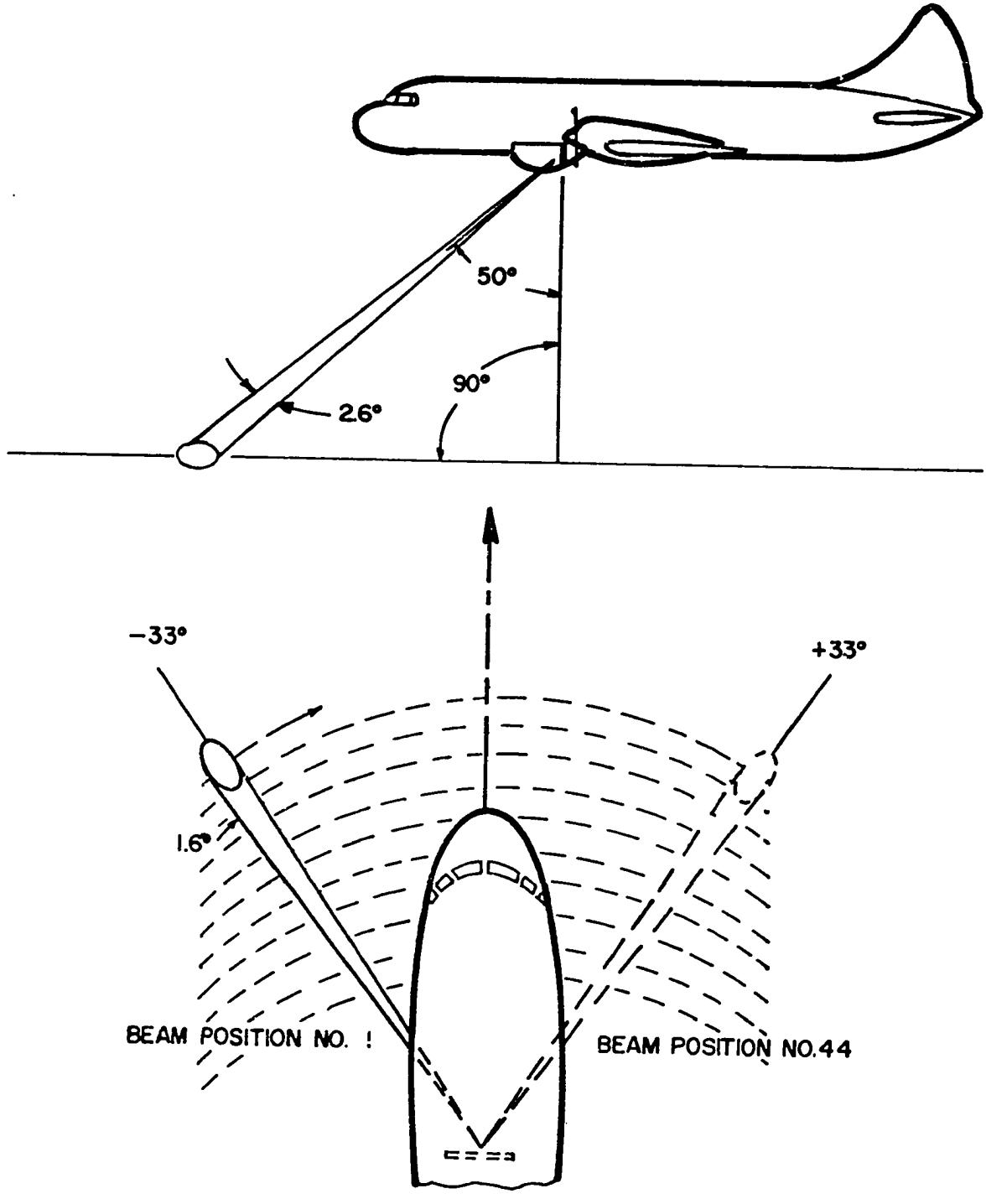

Figure 6. Sketch of the PMIS Scan Arrangement

signal from the radiometer is fed into the onboard computer to convert the readings to temperature in degrees Kelvin. An onboard television screen permits viewing of the image as the aircraft is flying, selective monitoring of individual data streams is provided, thus allowing the operator an opportunity to detect any malfunction in the equipment, and a camera is provided to photograph the onboard display.

Intermittent recording of data on tape is controlled by the operator without disrupting the onboard TV display. Experience has shown that up to 10 seconds may be required for internal temperatures in the onboard system to stabilize prior to recording acceptable data. Some unusually high temperatures may be stored on the first few scan lines, thus, as with most microwave systems, a warm up time or stabilizing time should be allowed prior to reaching the point where measurements are desired.

PCM tapes from the onboard recorder are converted to 9-track digital tapes at Houston using a data analysis system designed especially for this sensor (Fig. 7). No corrections are made in the data for cross polarization effects between the horizontal and vertical temperatures. Minor corrections are made in the system to compensate for radome and antenna losses associated with each individual beam position. Prior to this experiment, the only set of data available for the PMIS imager over land was the mission flown to perform evaluation of the equipment itself, thus, programs to appropriately display and analyze this data were not available for water resources studies. Programs are available at the Johnson Space Center (JSC) to display the data in a visual form on a color TV console thus allowing an investigator to scan

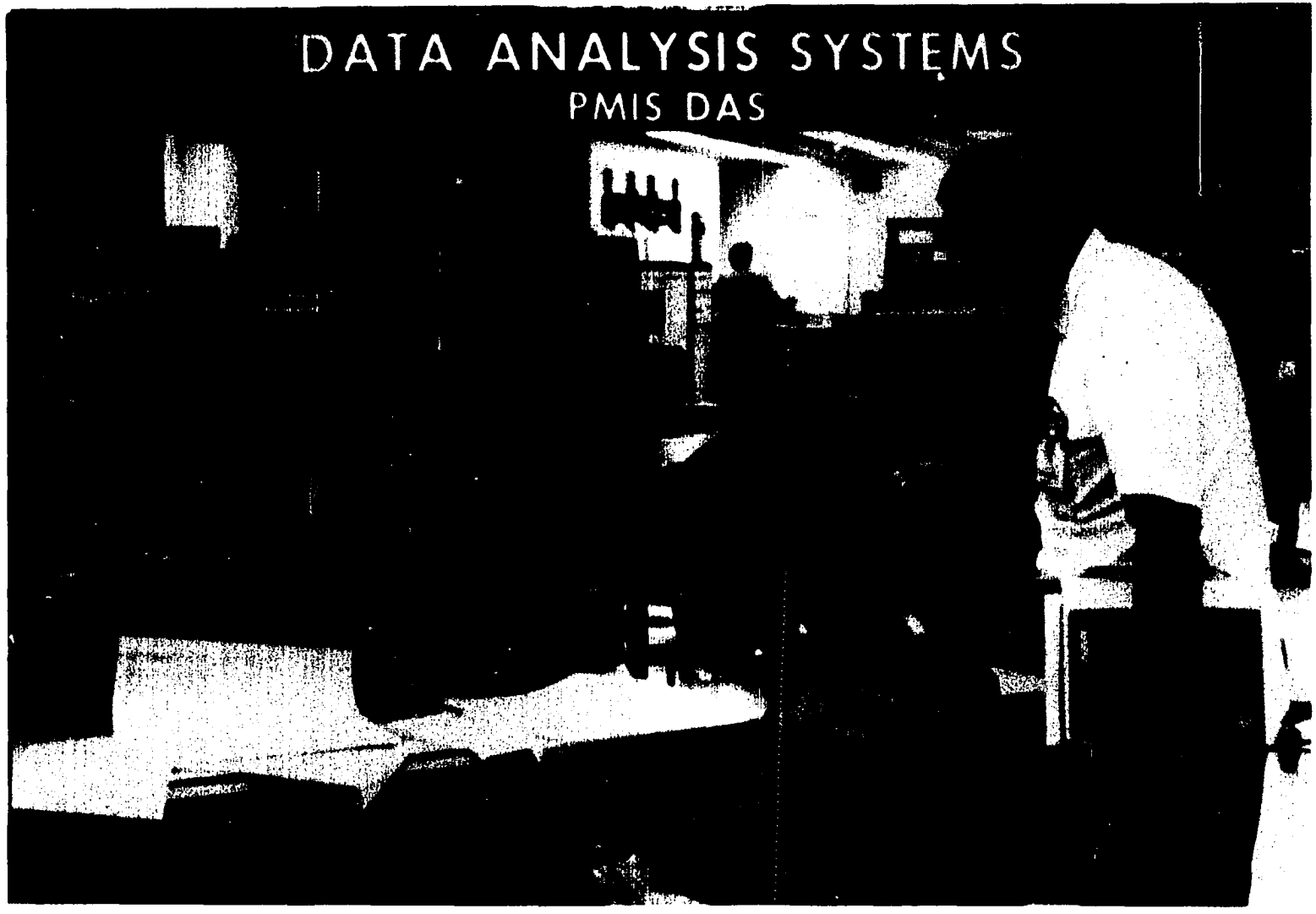

Figure 7. Photograph of Data Analysis System Console

his data and perform some cursory examination prior to working with the digital data itself.

The system scans a path on the surface approximately 1.25 times the absolute altitude of the aircraft. The X and Y coordinates of each beam position on a horizontal plane surface are calculated as the data are processed in the onboard computer system. Output on the 9-track computer tape gives the aircraft parameters; pitch, roll, altitude, speed, etc. (Fig. 8) for each scan line along with the X and Y components, vertical polarization temperatures, and horizontal polarization temperatures at each beam position.

Average temperatures in both polarizations for beam positions associated with the points within a watershed boundary were desired for this study. To simplify data processing, altitudes were requested that would allow the scan width to exceed the width of the watershed, thus, the antenna temperatures for a single watershed could be obtained from a single flight line. All flight lines were oriented lengthwise with each watershed and each was flown in an upstream direction. The flight configuration was intended to control effects of surface slopes on the antenna temperatures and for the watersheds in this test area, the influence of watershed slopes would be negligible.

Eight watersheds ranging in size from 1.46 to 16.45 square kilometers were selected for this study. Five are subwatersheds of East Bitter Creek, a tributary of the Washita River, and are located approximately 8 miles east of Chickasha, Oklahoma (Fig. 9). These five watersheds are located near the center of a large outcrop of the Chickasha formation, a part of the Permian Redbed. Soils derived from this

SCAN	TIME	LATITUDE	LONGITUDE	ALT-R	ALT-B*	HDN	VEL	VVEL*	PITCH	DRIFT	ROLL	DATE	MID	SITE	FLT	LINE	RUN
0029	16 29 26	+35/24.0	-098/22.0	10740	37600	270	241	2250	+01.3	-01.2	-00.8	04/28/73	227	184	02	08	01

T	2849	2849	2988	1841	3732	2794	2819	2797	2794	2984	2955	4032	4025	3333	3329	3289	3297	3284	3275	3211		
BM	1	2	3	4	5	6	7	8	9	10	11	12	13	14	15	16	17	18	19	20	21	22	CALS
V	2558	2695	2754	2758	2759	2771	2773	2769	2780	2796	2788	2749	2756	2768	2784	2761	2741	2740	2728	2771	2768	2777	0160
H	2479	2556	2630	2608	2642	2644	2621	2613	2608	2653	2607	2630	2592	2584	2639	2630	2614	2553	2523	2591	2658	2648	0166
X	0254	0255	0258	0260	0262	0281	0283	0285	0270	0272	0273	0274	0275	0277	0278	0279	0280	0280	0281	0282	0282	0283	
Y	0001	0001	0003	0007	0010	0010	0013	0017	0024	0027	0031	0034	0037	0041	0045	0048	0051	0055	0058	0062	0065	0069	
RL	-007	-007	-007	-007	-007	-007	-007	-007	-007	-008	-008	-008	-008	-008	-008	-008	-008	-008	-008	-008	-008	-008	

BM	23	24	25	26	27	28	29	30	31	32	33	34	35	36	37	38	39	40	41	42	43	44	BASE
V	2764	2791	2770	2774	2775	2767	2790	2746	2771	2755	2753	2740	2743	2748	2771	2749	2752	2733	2747	2737	2760	2743	0045
H	2647	2635	2629	2624	2636	2631	2604	2615	2630	2615	2598	2568	2585	2601	2641	2638	2648	2623	2616	2637	2634	2662	0044
X	0284	0284	0284	0284	0284	0284	0284	0284	0283	0282	0282	0281	0281	0280	0278	0277	0276	0274	0273	0271	0269	0267	
Y	0072	0076	0080	0083	0086	0090	0093	0097	0100	0104	0108	0111	0115	0118	0122	0125	0129	0132	0135	0139	0143	0146	
RL	-008	-008	-008	-008	-008	-008	-008	-008	-008	-008	-008	-008	-008	-008	-008	-008	-008	-008	-008	-008	-008	-008	

SCAN	TIME	LATITUDE	LONGITUDE	ALT-R	ALT-B*	HDN	VEL	VVEL*	PITCH	DRIFT	ROLL	DATE	MID	SITE	FLT	LINE	RUN
0030	16 29 28	+35/24.1	-098/22.3	10700	37600	270	241	2250	+01.3	-01.1	-00.8	04/28/73	227	184	02	08	01

T	2849	2849	2988	1841	3732	2794	2819	2797	2794	2984	2955	4032	4025	3333	3329	3289	3297	3284	3275	3211		
BM	1	2	3	4	5	6	7	8	9	10	11	12	13	14	15	16	17	18	19	20	21	22	CALS
V	2526	2728	2754	2791	2769	2771	2773	2759	2791	2807	2788	2760	2777	2758	2774	2782	2814	2750	2791	2812	2788	2788	0159
H	2452	2602	2648	2655	2689	2663	2641	2613	2608	2603	2587	2630	2623	2674	2659	2650	2634	2635	2636	2635	2628	2658	0166
X	0263	0265	0268	0270	0272	0274	0276	0278	0280	0281	0283	0284	0285	0287	0288	0289	0290	0290	0291	0291	0292	0293	
Y	0001	0001	0004	0007	0011	0014	0018	0021	0024	0028	0031	0034	0038	0042	0045	0048	0052	0055	0058	0062	0066	0069	
RL	-008	-008	-008	-008	-009	-009	-009	-009	-009	-009	-009	-009	-009	-009	-009	-009	-009	-009	-009	-009	-009	-009	

BM	23	24	25	26	27	28	29	30	31	32	33	34	35	36	37	38	39	40	41	42	43	44	BASE
V	2785	2791	2801	2795	2796	2778	2790	2788	2782	2787	2796	2761	2765	2769	2792	2781	2784	2722	2757	2758	2756	2774	0045
H	2626	2655	2629	2684	2656	2641	2685	2665	2660	2655	2648	2628	2664	2669	2669	2694	2686	2652	2634	2664	2662	2688	0044
X	0293	0293	0293	0293	0293	0293	0293	0292	0292	0291	0290	0290	0290	0289	0287	0286	0285	0283	0281	0280	0278	0276	
Y	0072	0076	0080	0083	0087	0090	0094	0097	0101	0104	0108	0111	0115	0118	0122	0125	0129	0132	0136	0139	0143	0146	
RL	-009	-009	-009	-009	-009	-009	-009	-009	-009	-009	-008	-008	-008	-008	-008	-008	-008	-008	-008	-008	-008	-008	

Notes: *-Instruments not recording properly in this sample data.
T-Temperatures for thermistors, degrees Kelvin x 10.
BM-Beam positions along scan line.
V-Vertical polarization temperature, degrees Kelvin x 10.
H-Horizontal polarization temperature, degrees Kelvin x 10.
X-Position of beam along flight line.
Y-Position of beam from left edge of scan.

Figure 8. Typical Computer Printout of PMIS Data

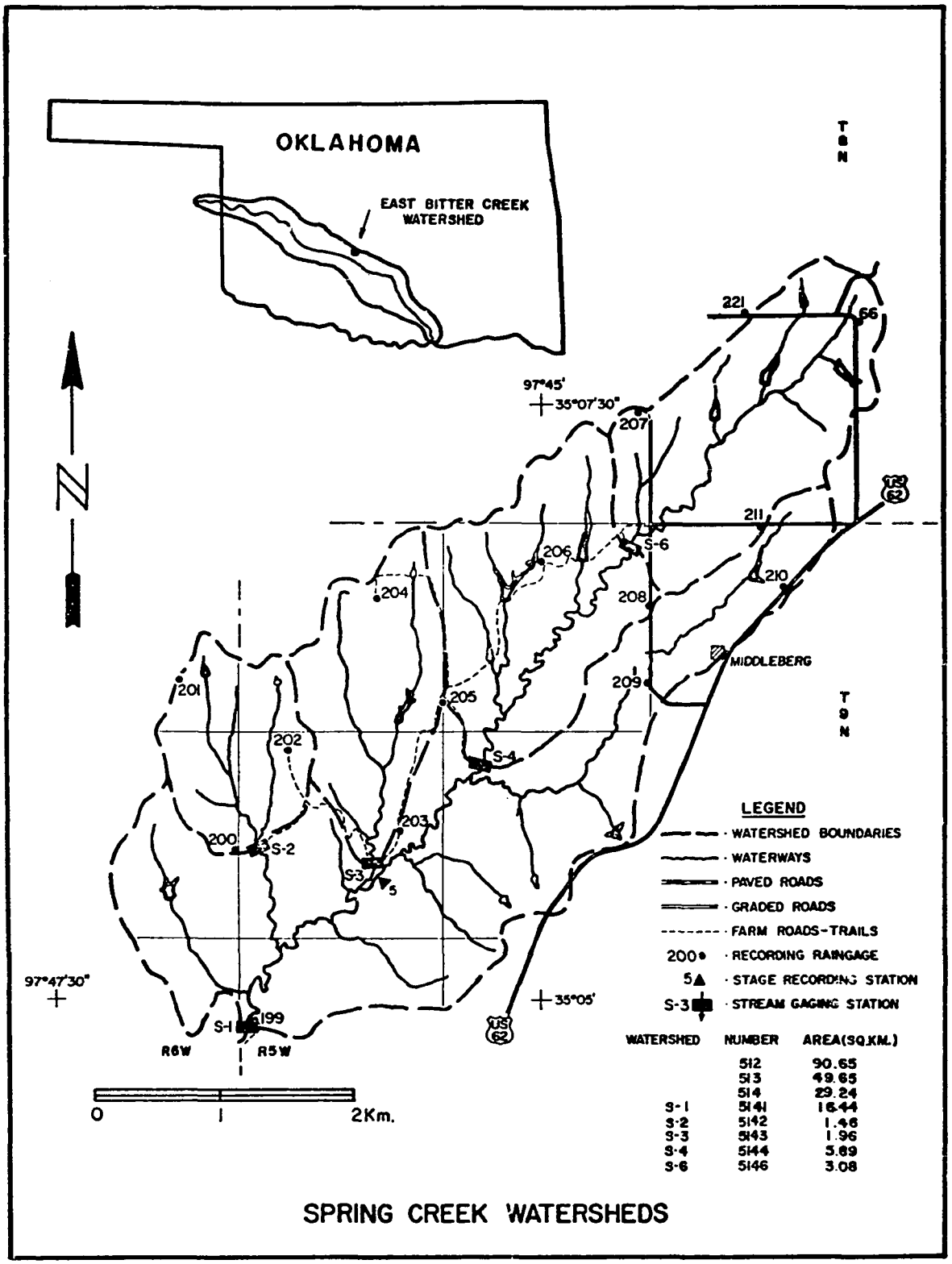

Figure 9. Map of Spring Creek Watersheds

formation are medium to low permeability and devoted to production of native grass pastures. Areas within these watersheds that were once cultivated have very little top soil remaining and native grass stands are consequently poor. Runoff from these watersheds is relatively high for the region. Three of the watersheds, 5141, 5142, and 5144 produce low flow throughout most of the year when rainfall is near normal, while watersheds 5143 and 5146 have ephemeral stream channels.

Three subwatersheds on Sugar Creek located near Lookeba, Oklahoma (Fig. 10) were selected to represent low runoff areas. The geologic base of these watersheds is the Rush Springs Sandstone, another outcrop of the Permian Redbed. The soils in this area are sandy, more permeable and subject to severe erosion. Steep slopes are timbered pasture while more gentle slopes near the top of the watershed are devoted to production of peanuts and maize. One of the watersheds, No. 25, has a long narrow basin with a sandy timbered alluvium extending two-thirds the length of the watershed.

The eight watersheds selected are all instrumented with weighing recording rain gages. Runoff from the five watersheds on East Bitter Creek is measured by calibrated V-notch weirs, while runoff on the three Sugar Creek watersheds is calculated from water stage recorders on carefully surveyed flood detention ponds. The eight watersheds are representative of the range of runoff conditions experienced in central Oklahoma. A record of water levels was available for a sample of the farm ponds within each drainage area for the years of record, thus, an estimate of drainage area for each storm runoff event could be made.

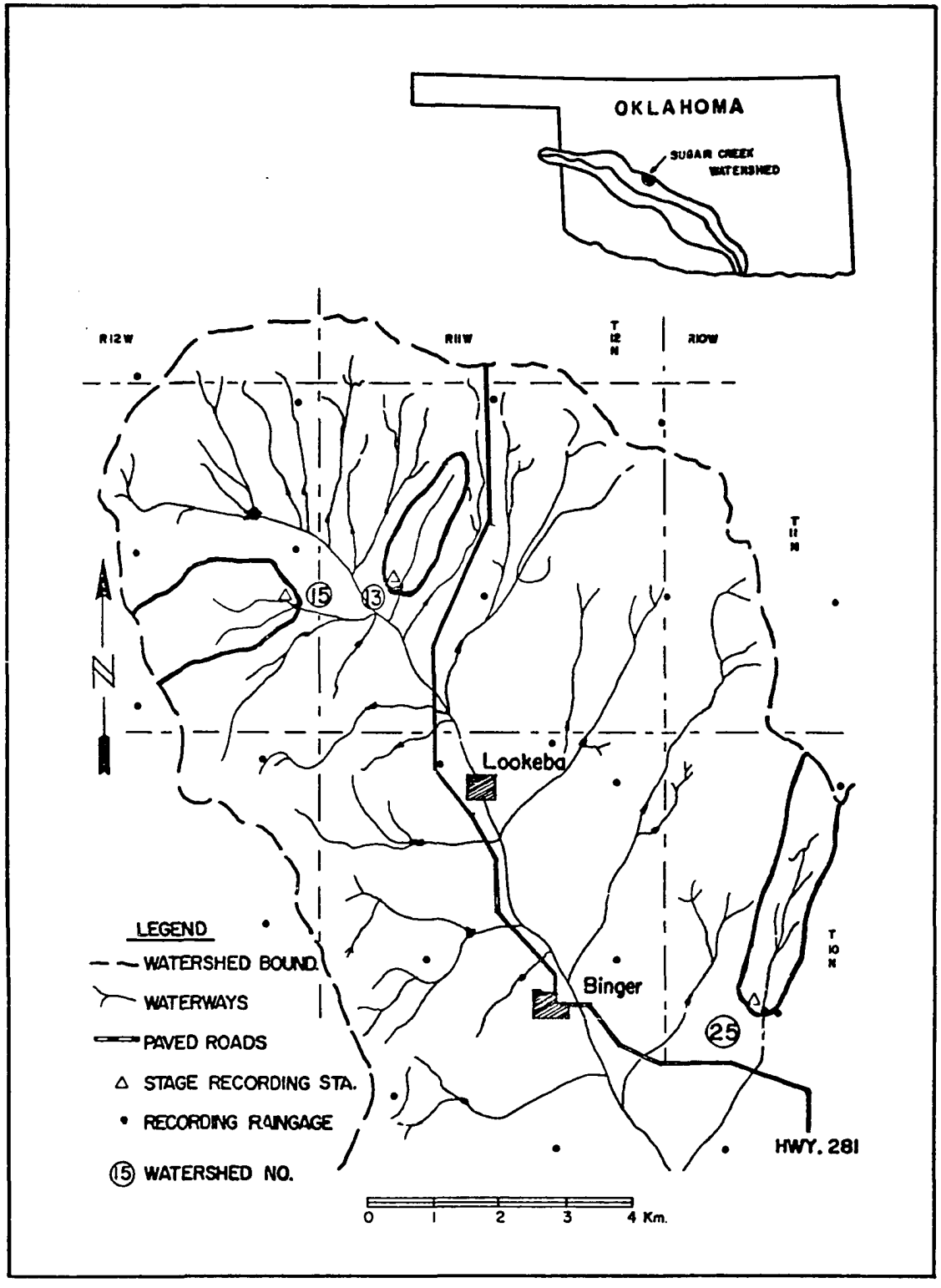

Figure 10. Map of Sugar Creek Watersheds

The two watershed variables selected for comparison to passive microwave measurement were: (1) The adjusted mean annual runoff (cm/yr) for mean annual rainfall, and (2) the coefficient (CN) used in the Soil Conservation Service (SCS) storm runoff equation. Numerous other storm runoff equations are available (Chow, 1964). Selection of the above variables was based first on the fact that both values are presently in common use by practicing hydrologists and secondly, either or both might conceivably be related to microwave emissions. Mean annual yield prediction is important for municipal water supply and the SCS equation is most commonly used at this time in design of flood detention structures on watersheds of this size.

This experiment was planned to merely determine if average microwave temperatures from the watershed surface might be related to runoff producing capability of the watersheds. Due to extreme costs of data collection and processing and the fact that this concept had not been laboratory tested, it appeared impractical to select enough watersheds to produce statistical confidence in the results. The plan in general was to collect passive microwave vertical and horizontal polarization temperatures, surface temperatures, and photographs to verify location of the aircraft over the eight watersheds on two consecutive flights. One flight would represent wet conditions and another for measurement during dry conditions. Time between flights should not allow major changes in vegetative growth, and weather conditions for both flights should be clear.

Average microwave temperatures, differences in dry and wet temperature and differences in vertical and horizontal temperatures will be compared graphically to average annual runoff (centimeters/year) and the storm runoff equation coefficient (CN).

CHAPTER V

PROCEDURE AND DATA PROCESSING TECHNIQUES

Watershed Data

The hydrologic data on the eight watersheds used in the study had been collected by the Southern Great Plains Research Center at Chickasha, Oklahoma in connection with other studies. A primary network of rain gages covering a two-county area provide rainfall records. Weighing-type rain gages are located in a rectangular grid pattern with approximately 48 km. spacing between gages.

Five of the watersheds located within the drainage area of East Bitter Creek are instrumented with additional gages, each watershed having a minimum of three gages spaced around the watershed boundary. Runoff from each watershed in this group is measured by concrete V-notch weirs calibrated by standard stream gaging and laboratory modeling methods. Farm ponds above the runoff stations are equipped with staff gages which are read on a regular weekly basis with additional readings at the end of each runoff event. The collection of rainfall and runoff records on these five watersheds began in 1966 and is considered of excellent quality.

The remaining three watersheds located on Sugar Creek near Lookeba, Oklahoma are used in a current study of sediment delivery into SCS flood detention reservoirs. Each watershed drainage network terminates at a

flood detention structure equipped with an A-35 Stevens stage recorder activated by a gas-operated bubbling manometer. Detailed surveys were made of the storage basin from which stage volume curves are derived. Runoff on these watersheds is calculated from change in volume and may be a poor estimate for small storms, but is acceptable for large storms. Losses to seepage and bank storage in these watersheds would be significant, but is not accounted for in records of this nature.

Rainfall records for the three Sugar Creek watersheds were obtained from the existing 4.8- by 4.8 km. grid network of recording rain gages. Storm events selected for use in this study were limited to those events having more than .025 centimeters of runoff from the watershed surface and more than 2.54 centimeters of Theissen weighted rainfall. The period of record represented some extremely low rainfall years and small storm events are plentiful while only two or three large events occurred on each watershed. Also, due to the generally dry conditions in the period of record, very few events occurred when antecedent rainfall was high. All events that were used fell in the SCS antecedent moisture classifications of I or II, having a 5-day antecedent rainfall less than 2.79 centimeters in the dormant season or 5.33 centimeters in the growing season.

Farm pond storage controls flow from a very small percent of the drainage area for the three Sugar Creek watersheds. Soils with more than 10 percent clay content are not available in the area, thus many of the farm ponds that were built in the past failed soon after construction and have not been replaced. One watershed in the East Bitter Creek group also had a low percentage of area above farm ponds.

It was found that the percentage of drainage area above farm ponds varied from 4.31 percent to 38.0 percent for the sample watersheds. An adjustment in the drainage area contributing to measured runoff was necessary to compensate for the difference of pond storage effects on the individual watersheds. Stage records on farm ponds were used to estimate the percentage of the area above farm ponds that actually contributed some runoff to the watershed storm discharge. The recorded runoff was then attributed to the area below ponds plus any estimated contributing area from above the ponds. Very little farm pond overflow was recorded during the period of record available, and, for the majority of storms, the contributing drainage area was essentially that portion of the watershed below farm ponds.

Using the weighted storm rainfall and the adjusted runoff as input, a simple iterative type calculation was programmed in Fortran language to calculate the Soil Conservation Service runoff equation coefficient (CN). A coefficient was calculated for all selected storms for each watershed. The coefficients were then averaged to arrive at a single coefficient that would represent the average response of the watershed. It is recognized that the coefficient in a simple empirical equation using only storm rainfall as input will vary with changes in other variables such as season, intensity or duration of rainfall, changes in vegetative cover or tillage, and possibly, direction of storm movement over the individual watershed. A large number of storms would be necessary with all but one of these variables relatively stable to define a more precise coefficient appropriate to the time the watersheds were overflown. Records available for these watersheds provide data for no more than 20

storm events for a single watershed with the majority occurring in the spring and fall months. Coefficients calculated in the above manner are therefore limited by the amount of data available and should be recognized as an approximation based on recorded rainfall and runoff. The calculated average coefficients are listed for each watershed in Table 1.

TABLE 1

WATERSHED CHARACTERISTICS

	Watershed Number							
	5141	5142	5143	5144	5146	13	15	25
Drainage Area (km^2)	16.45	1.46	1.97	5.92	3.08	5.15	9.92	8.11
% Area above Farm Ponds	22.8	7.28	33.4	38.0	29.2	5.49	4.31	8.13
Number of Rain Gages	17	3	4	9	6	3	3	2
Storm Runoff Coefficient (CN)	61.5	59.4	56.3	62.8	63.8	37.0	46.0	51.0
Average Annual Runoff (cm)	7.75	6.93	5.00	9.19	5.11	2.03	.884	1.24

Annual rainfall and annual runoff for all watersheds was calculated by merely summing published daily rainfall and summing runoff values that were adjusted to compensate for the portion of the drainage area that contributed as runoff due to farm ponds. In most years there was some expected deviation in annual rainfall from the "normal" average rainfall. There was, however, considerable difference in annual rainfall between each group of watersheds. Lower annual rainfall generally occurred over the Sugar Creek watersheds. In order that influence of

varying input to the watershed would not bias the yield values, all annual runoff values were adjusted by multiplying them by a ratio of the estimated mean annual rainfall (78.74 cm/year) divided by measured annual rainfall. A straight line relation between annual rainfall and annual runoff was assumed. Such an adjustment does not necessarily remove all the variation in runoff created by variation in annual rainfall, however it is difficult to define the complex interaction of other variables in the rainfall-runoff relation. The definition of the more complex relation between annual rainfall and annual runoff was considered beyond the scope of this investigation. Mean annual runoff values were calculated after each annual runoff value was adjusted to the mean annual rainfall. The mean annual runoff values are also listed as part of Table 1.

Microwave Data

Two sets of data were processed from the NASA passive microwave imaging system (PMIS), one collected on Mission 227, April 28, 1973, and the second collected on Mission 235, June 25, 1973. The April mission was flown when the watersheds were relatively wet, while the June 25 mission was flown under dry conditions. Antecedent precipitation index (Linsley, et al., 1949) values ranged from .305 to .371 for the April mission and .160 to .199 for the June mission. The data from both missions consisted of 9-track tapes of digital imager data, digital tapes and printed tabs of the surface temperature along the flight lines, measured by the PRT5 far infrared sensor aboard the aircraft, and both color and color infrared 9-inch positive transparencies with overlapping coverage along the flight track.

The PMIS data on 9-track tapes contains values for instrument parameters that were not pertinent to this study. A listing of the word locations (Appendix A) shows some data listed that is used for analysis of system performance and was not needed for this study. The data tapes were read (Program 1, Appendix A) on an IBM 360 system and only the data necessary for the study; scan number, beam position number, vertical polarized temperature, horizontal polarized temperature, X and Y coordinates of the beam position, flight line and run numbers, were punched on cards. Each card contained data for two consecutive beam positions, thus requiring 22 cards per scan line. The listing of word locations for data in the tape format gives no indication that reformating from the tape to cards would be difficult, however, the real values of both vertical and horizontal temperatures in degrees Kelvin were found to be stored on the tapes as integers 32 times larger than the real values while printouts produced when the 9-track tape is loaded show the temperature as real values of the right order.

Imager data on cards was then stored on disk files for an IBM 1130 computer equipped with a 30-inch roll type plotter. Each flight line and run was stored as a matrix file readily available for plotting, corrections, or extraction of data points related to a watershed area.

Initial plotting of the files revealed that occasional data points were misplaced on the plots. During the flights, static had been detected on the onboard TV screen, apparently caused by UHF radio transmission during data collection. Examination of the misplaced data points revealed that the vertical and horizontal temperatures were not affected by the interference, but the X and Y coordinates are calculated using

output from a radar altimeter and this equipment was apparently being influenced by radio transmissions. The error introduced in the imager stems from the fact that the onboard computer calculates an apparent higher altitude each time interference enters the radar altimeter. Each miscalculated X and Y coordinate then places the beam position farther out than it should be on a radial from the nadir point. Correction of the errors in coordinates were made on the cards after locating errors by plotting beam positions and then corrected disk files were recompiled. For future data processing the coordinate corrections could be more readily accomplished with a computer program since the distance between scan lines and distance between beam positions in the scan line remains relatively constant for a constant altitude.

As stated in the prior description of the equipment, no correction for effects of cross polarization are made by the data analysis system that generates the 9-track tapes. Data from a previous systems acceptance flight over Trinity Bay (McAllum, 1973) had indicated that corrections necessary for the outer beam positions would be quite large over low temperature targets. Temperatures over land are much higher and it appears that cross polarization effects diminish as temperatures increase (Fig. 11).

Corrections for cross polarization for this study were made by calculating two sets of dimensionless coefficients F_{v_i} and f_{h_i} (Equations 2 and 3) based on the assumption that the effect on both the vertical and horizontal temperatures for a specific beam position was a function of the difference in average temperature recorded for each polarization. Mean temperatures were calculated for each beam position for the entire

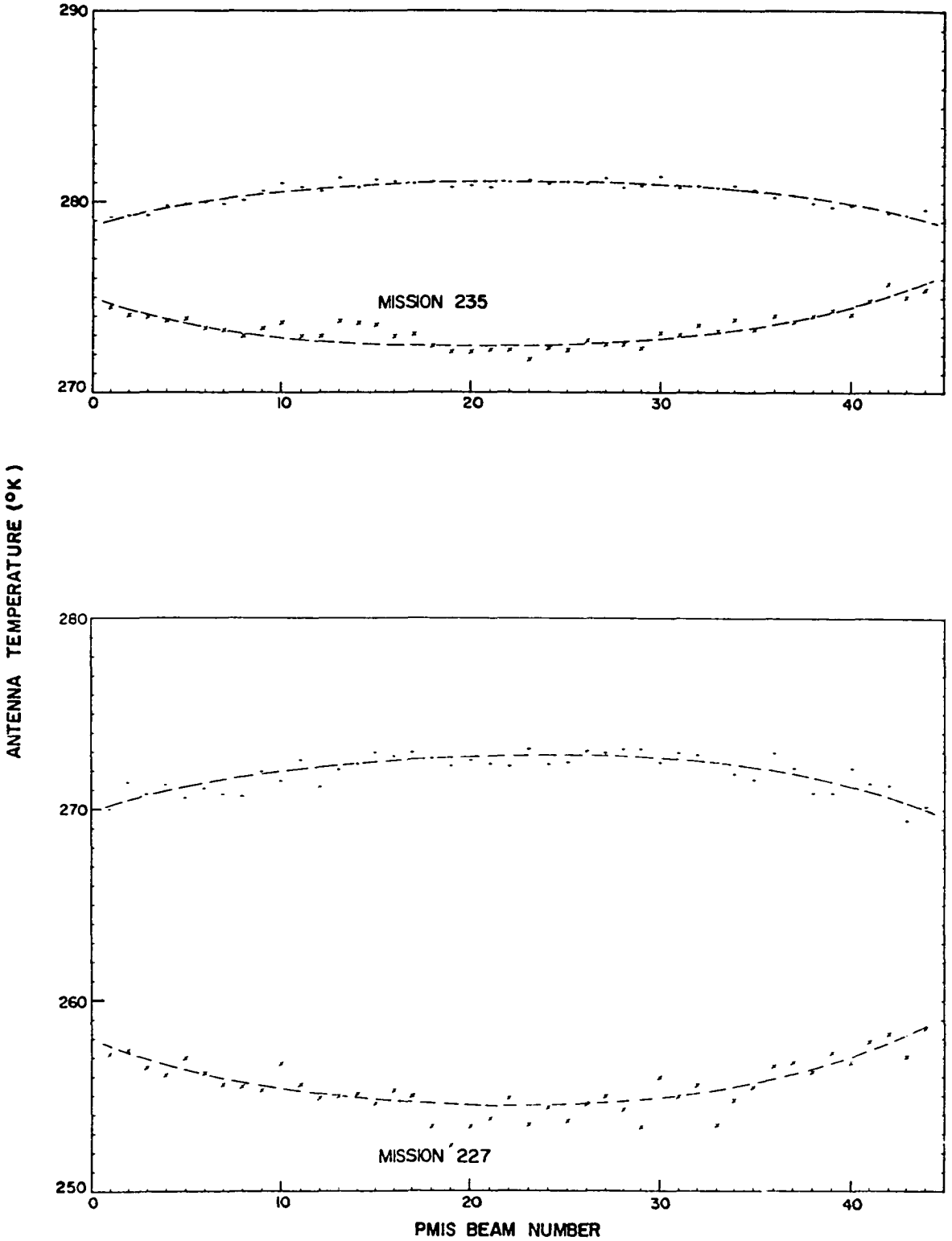

Figure 11. Illustration of Cross Polarization Effects

set of data collected for each mission (Program 2 and 2A, Appendix A), Coefficients based on the mean temperatures were then calculated for each mission (Program 3, Appendix A).

$$T_{v_{max}} = T_{v_i} + f_{v_i} (T_{v_i} - T_{h_i}) \quad (2)$$

$$T_{h_{min}} = T_{h_i} - f_{h_i} (T_{v_i} - T_{h_i}) \quad (3)$$

where $T_{v_{max}}$ = maximum average vertical temperature (°K)

$T_{h_{min}}$ = minimum average horizontal temperature (°K)

T_{v_i} = average vertical temperature at beam position i (°K)

T_{h_i} = average horizontal temperature at beam position i (°K)

The appropriate coefficients were then used to calculate a cross polarization correction for the antenna temperatures and rebuild the disk files of imager data (Program 4, Appendix A). This procedure might be more readily described as a technique to normalize the response to obtain the same temperatures at each beam position that would be recorded by the center beams if the aircraft had been centered over that particular strip of the image.

The color infrared positive transparencies for each flight line were combined in a mosaic and the boundary of the watershed was outlined on the mosaic. Each photo mosaic was then used as the base to which the microwave image plot could be matched.

The only outstanding feature of microwave temperatures over the watershed areas was the extreme low temperature sensed when the microwave beam fell on open water such as a pond. Ponds in flood detention

structures and some of the larger farm ponds were used as key positions to match the plotted temperatures with the photo mosaic.

Program 5, Appendix A was used to slice the microwave temperature into intervals where a letter code could be used to represent a temperature interval on the plotter (Fig. 12). A plot of the coded image can be generated in less time than a plot of the temperatures and the coded image was easier to interpret visually. A rough estimate of the plotter scale was calculated based on the estimated width of the microwave imager scan and the corresponding width on the photographs. Two or more ponds on each of several lines were then matched with low temperatures in the microwave images by enlarging or shrinking the plot with minor changes in scale to determine the constant scale appropriate for each mission.

Each flight line plot of the microwave temperature was matched to the mosaic of that flight line. The watershed boundary was transferred to the plotted overlay and for each scan line crossing a watershed boundary, beam positions immediately inside the watershed boundary were listed and punched on cards. The deck of cards was used as a control for a computer program (Program 6, Appendix A) that would search the disk file and compute averages for both vertical and horizontal polarized temperatures using only the data pertaining to points within the watershed. Average vertical and horizontal temperatures related to the watershed surface (Table 2) were calculated for each watershed for both flight dates.

Average passive microwave temperature for a surface is a function of surface temperature (Equation 1) and before two sets of microwave temperatures collected at different times from the same target are

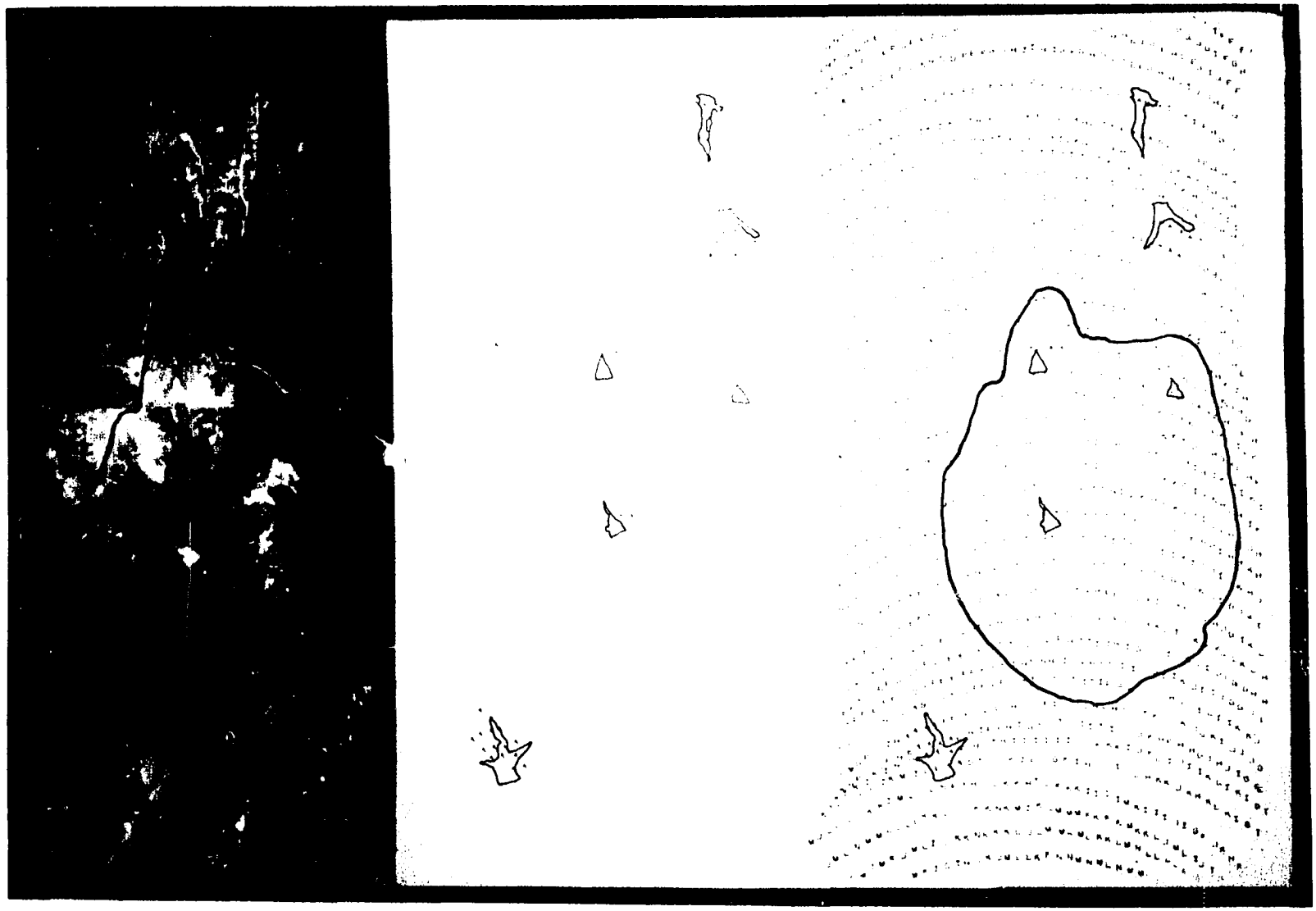

Figure 12. Mosaic of Watershed 5142 with Plotted Overlays

TABLE 2

SUMMARY OF MICROWAVE AVERAGE TEMPERATURES

	Watershed Number							
	5141	5142	5143	5144	5146	13	15	25
Number of Data Points	1,980	376	453	782	433	597	247	1,302
Mission 235								
Average Vertical Temperature (T_{v235}) °K	284.1	283.6	284.8	283.7	283.4	271.8	269.6	282.6
Average Horizontal Temperature (T_{h235}) °K	272.8	274.4	273.1	273.8	273.9	273.4	276.7	275.6
Average Surface Temperature (T_{g235}) °K	301.8	302.8	302.8	301.8	301.8	301.2	305.5	301.1
Mission 227*								
Average Vertical Temperature (T_{v227}) °K	276.6	281.1	273.7	274.9	276.3	279.0	286.8	278.8
Average Horizontal Temperature (T_{h227}) °K	251.8	252.0	252.4	253.4	247.9	262.2	271.2	260.8
Average Surface Temperature (T_{g227}) °K	297.3	298.7	298.7	297.3	297.3	296.4	294.1	296.4
Δv ($T_{v235} - T_{v227}$) °K	7.5	2.5	11.1	8.8	7.1	-7.2	-17.2	3.8
Δh ($T_{h235} - T_{h227}$) °K	21.0	22.4	20.9	20.4	26.0	11.2	5.5	14.8
235 ($T_v - T_h$) °K	11.3	9.2	11.7	9.9	9.5	-1.6	-7.1	7.0
227 ($T_v - T_h$) °K	24.8	29.1	21.5	21.5	28.4	16.8	15.6	18.0
Storm Runoff Coefficient (CN) Dimensionless	61.5	59.4	56.3	62.8	63.8	46.0	37.0	51.0
Adjusted Average Annual Runoff (cm.)	7.75	6.93	5.00	9.19	5.11	2.03	.884	1.24

*Temperatures adjusted to average watershed surface temperatures for Mission 235

compared, the difference in surface temperature must be accounted for. Average surface temperature for a line through the center of each watershed was readily available from the aircraft data (Table 2). Mission 227 average antenna temperatures can be converted to average antenna temperatures that would have occurred with ground temperatures recorded during Mission 235 by use of Equation 4. This equation is derived from Equation 1 for two different conditions of surface temperature, T_G, and holding the sky temperature, T_S, constant. Sky temperature in this instance was estimated to be 10°K. (Paris, 1974).

$$T_{A_2} = \left[\frac{(\overline{T}_{A_1} - 10)}{(\overline{T}_{G_1} - 10)} (T_{G_2} - 10)\right] + 10 \qquad (4)$$

where T_{A_1} = recorded average antenna temperature, Mission 227

T_{G_1} = recorded average surface temperature, Mission 227

T_{G_2} = recorded average surface temperature, Mission 235

T_{A_2} = equivalent average antenna temperature

A summary of the measured average antenna temperature for Mission 235 and calculated average antenna temperatures for Mission 227 based on Mission 235 surface temperature for each watershed is presented in Table 2. Differences between vertical and horizontal polarized temperature for each mission and differences between like polarized temperatures between the "wet" 227 Mission and the "dry" 235 Mission are listed in the same table. Also, the watershed annual runoff in centimeters and the calculated average runoff coefficient (CN) are listed again for convenience since these values are used in the following plots.

Figures 13 through 20 were plotted from the summary in Table 2 to determine if any relationship exists between the passive microwave temperatures and either watershed storm runoff or annual yield.

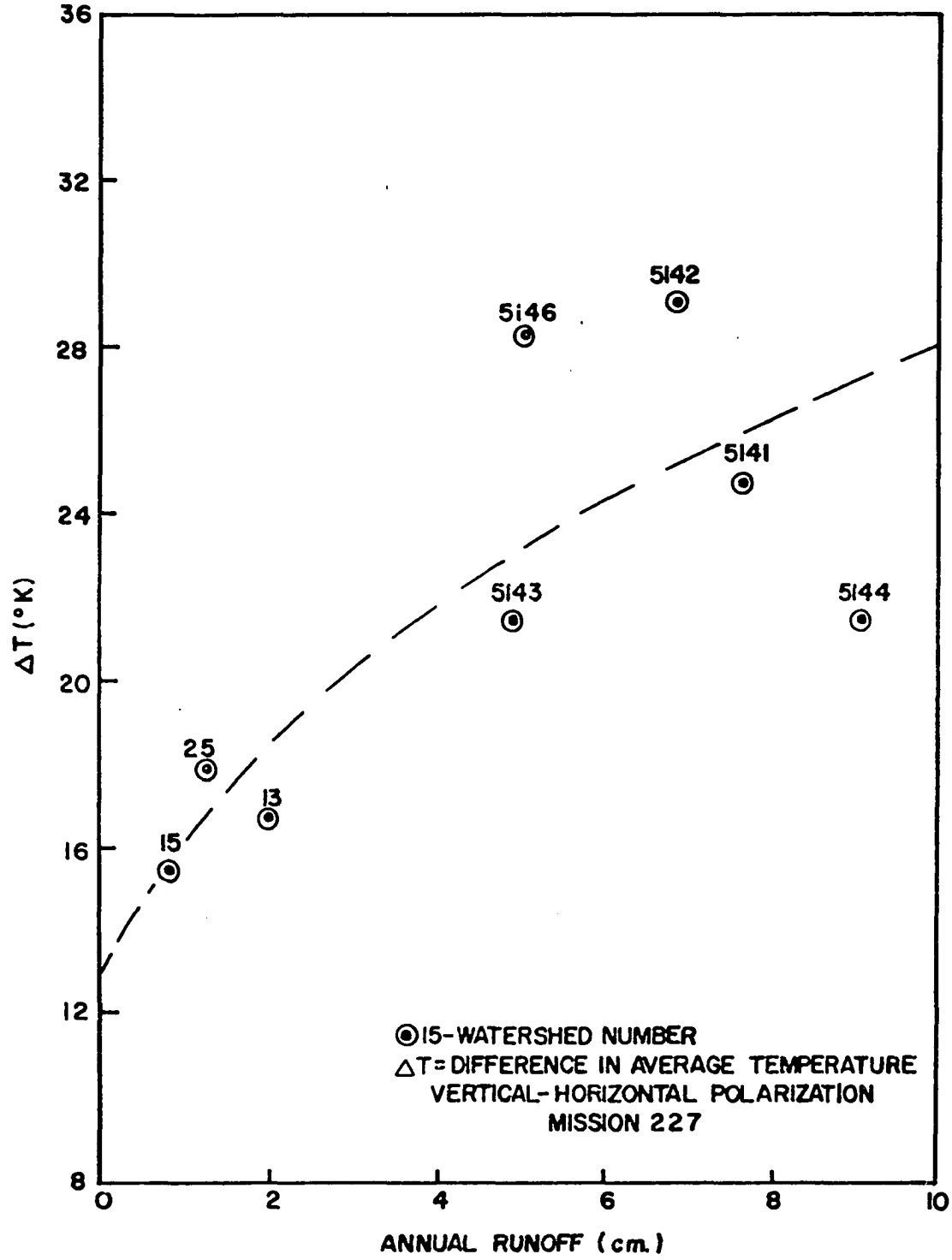

Figure 13. The Relationship between Vertical and Horizontal Temperature Differences in April and the Annual Watershed Runoff

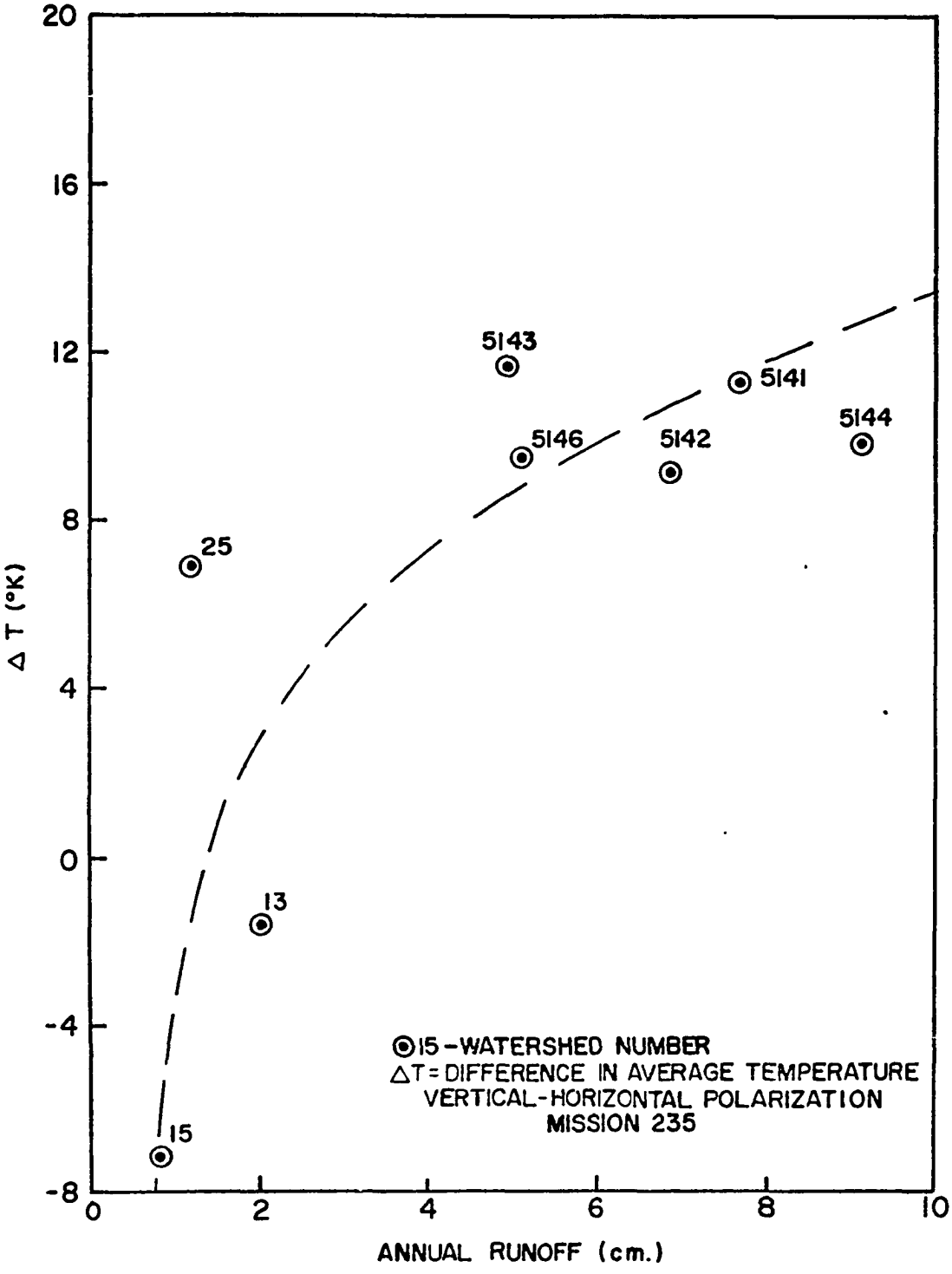

Figure 14. The Relationship between Vertical and Horizontal Temperature Differences in June and the Annual Watershed Runoff

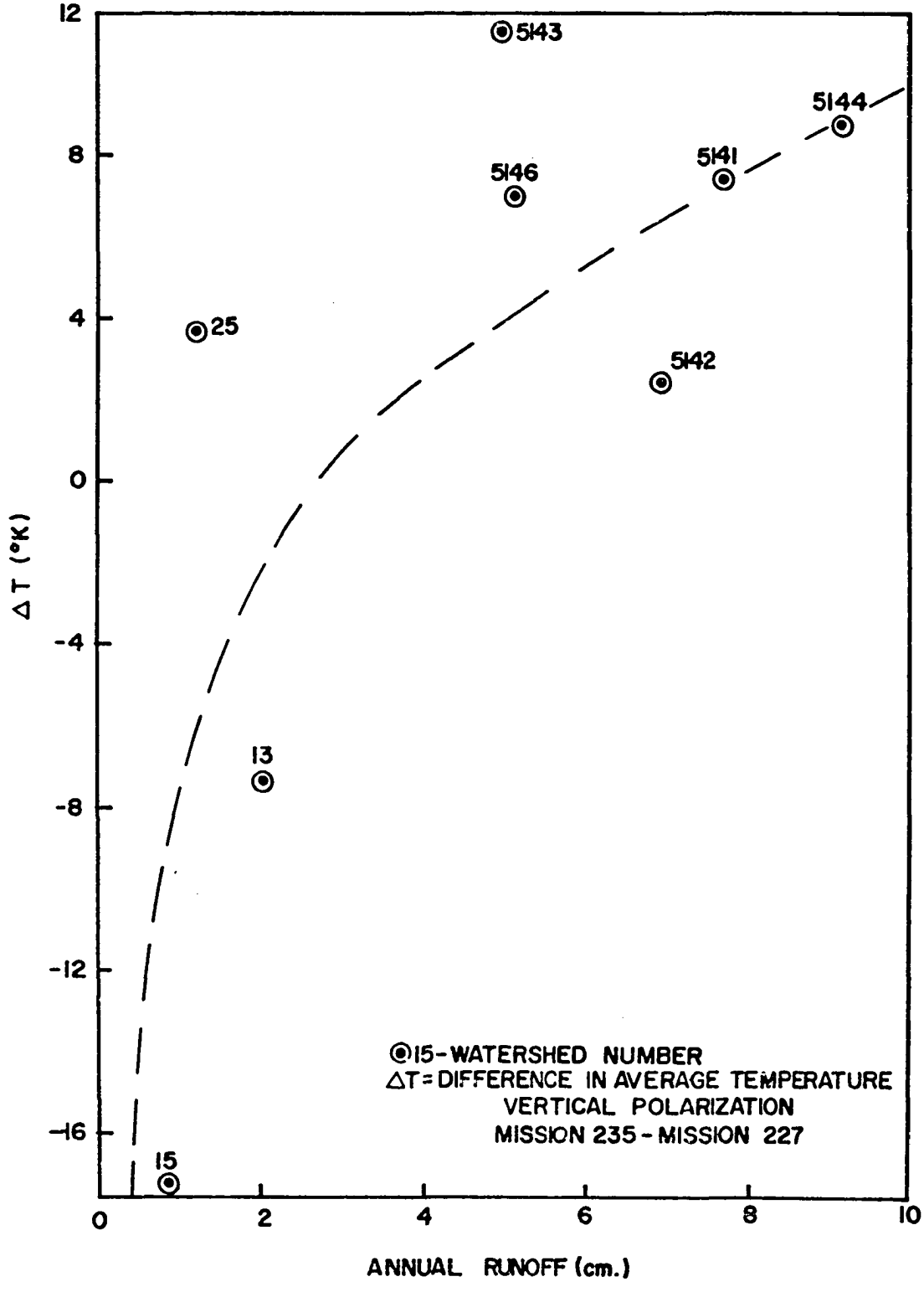

Figure 15. The Relationship of Differences in Vertical Polarized Temperatures from Two Flights to the Annual Watershed Runoff

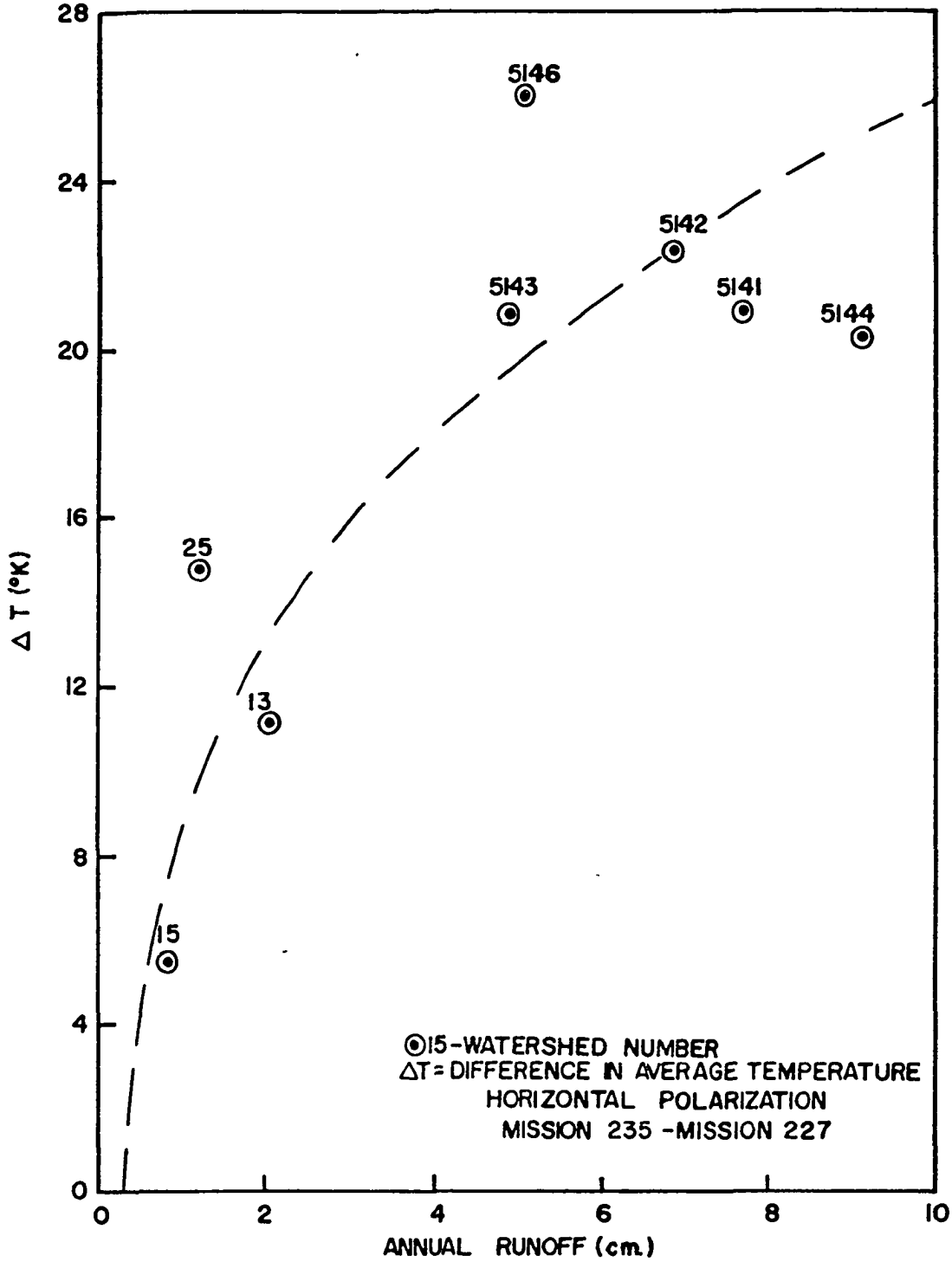

Figure 16. The Relationship of Differences in Horizontal Polarized Temperatures from Two Flights to the Annual Watershed Runoff

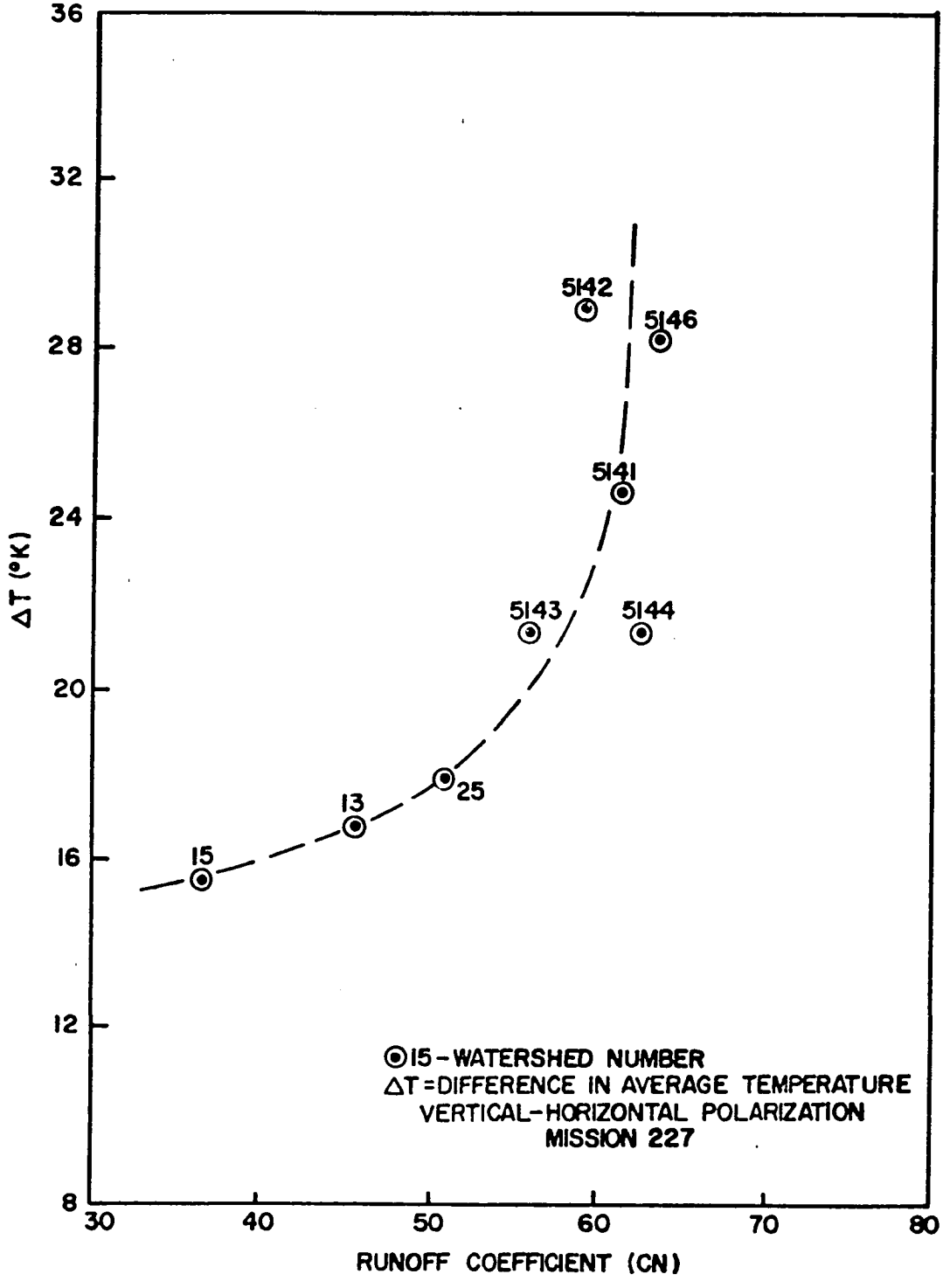

Figure 17. The Relationship between Vertical and Horizontal Temperature Differences in April and the Watershed Storm Runoff Coefficients

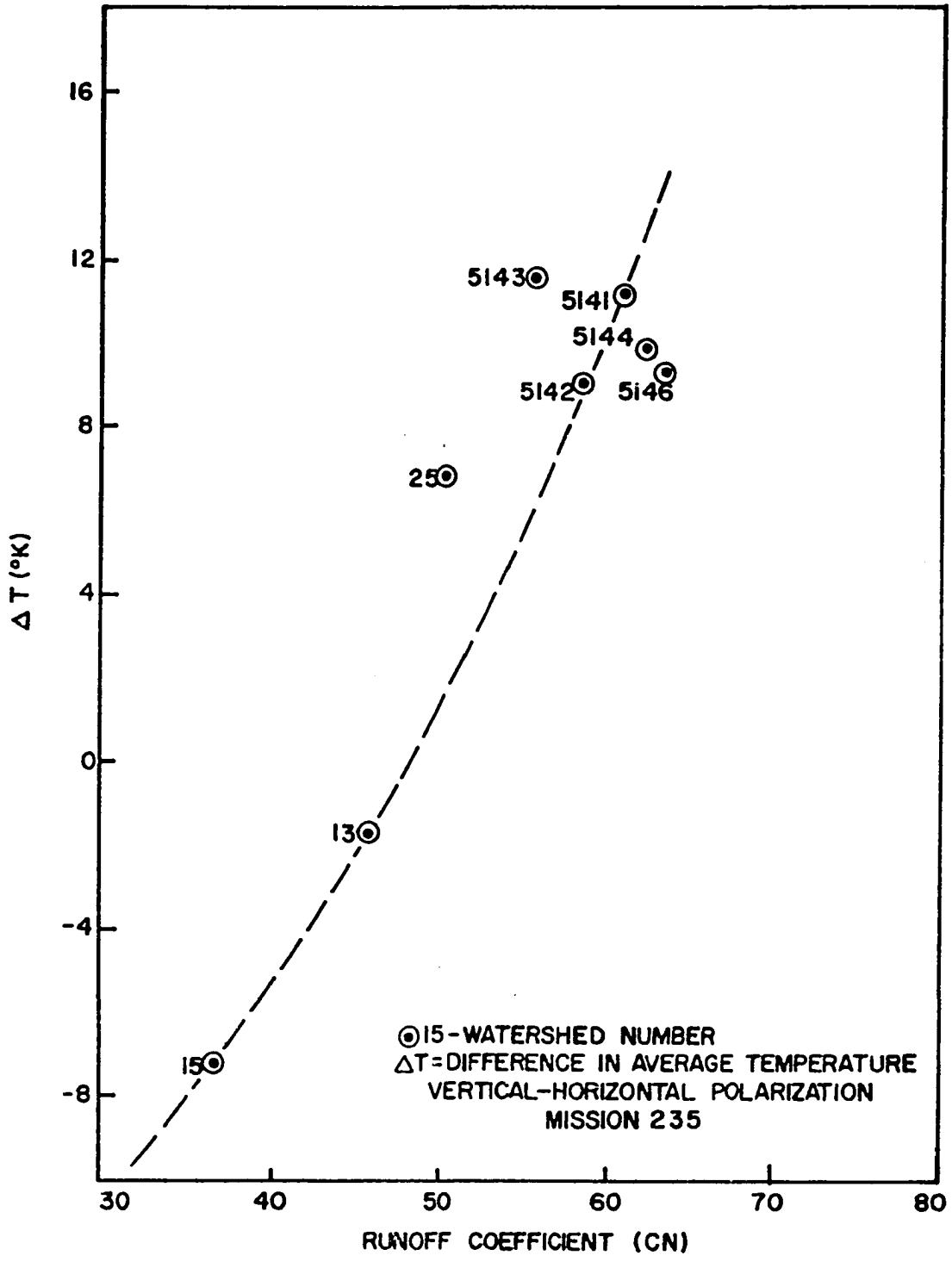

Figure 18. The Relationship between Vertical and Horizontal Temperature Differences in June and the Watershed Storm Runoff Coefficients

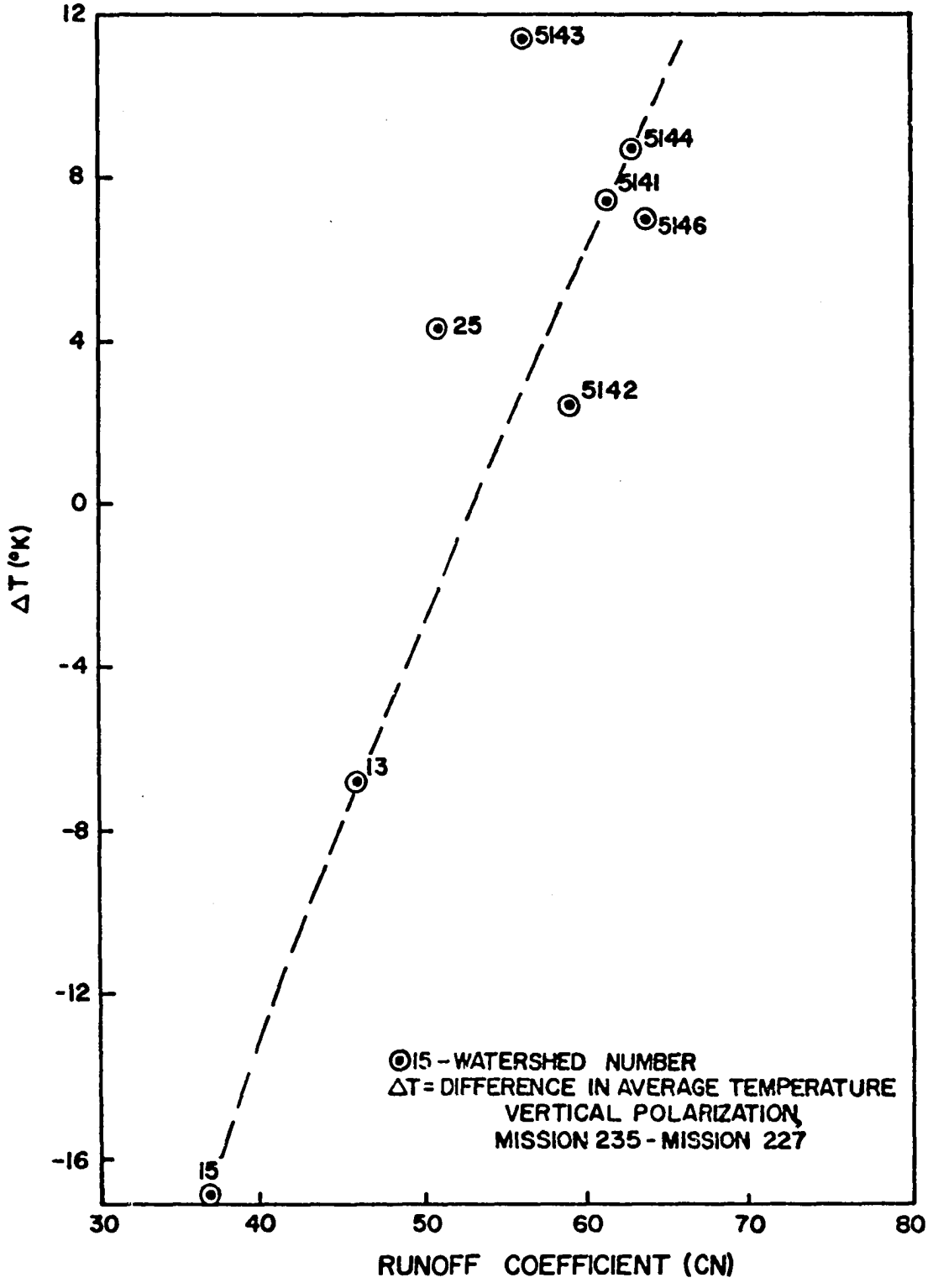

Figure 19. The Relationship of Differences in Vertical Polarized Temperatures from Two Flights to the Watershed Storm Runoff Coefficients

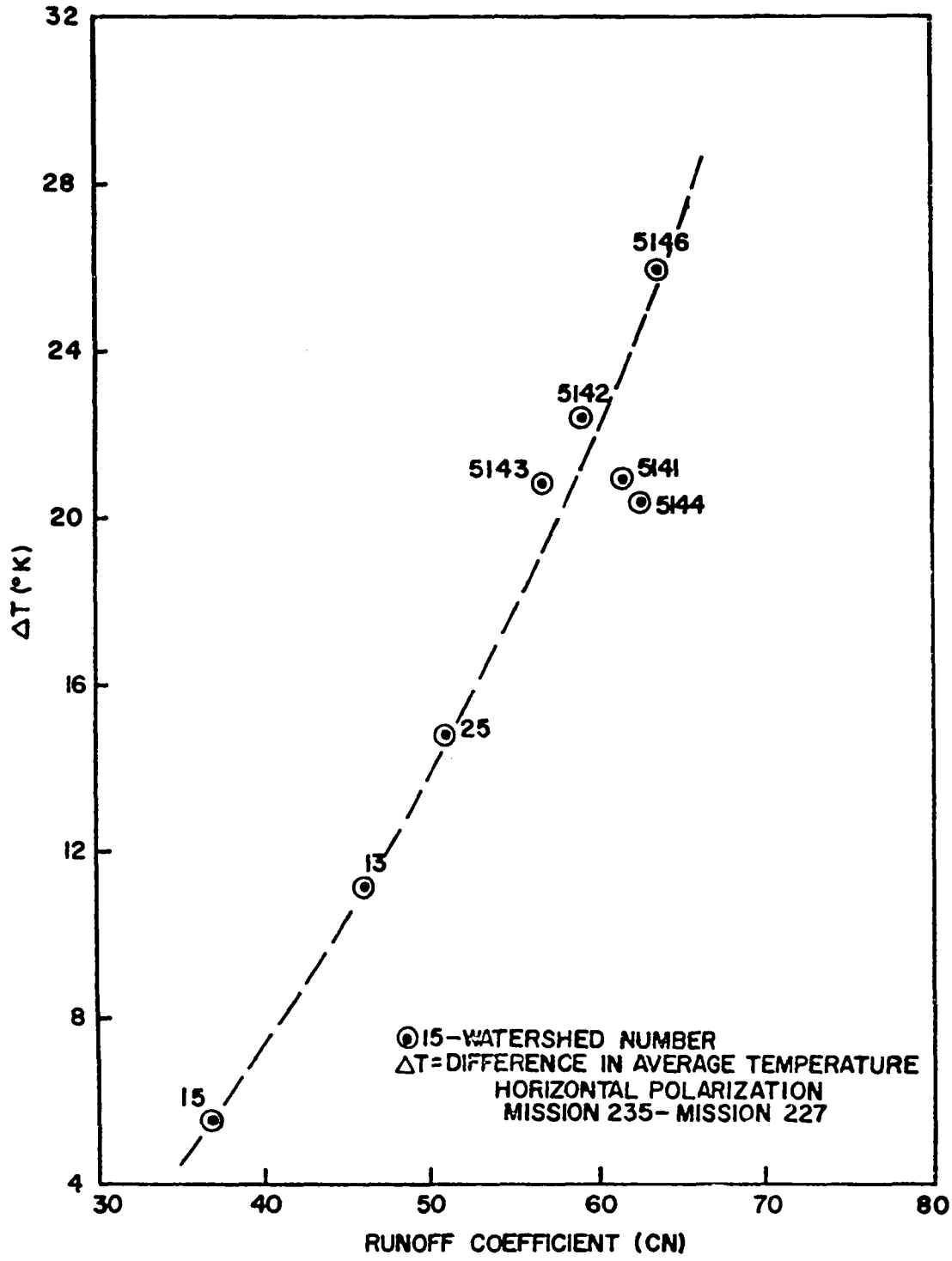

Figure 20. The Relationship of Differences in Horizontal Polarized Temperatures from Two Flights to the Watershed Storm Runoff Coefficients

CHAPTER VI

DISCUSSION AND RESULTS

A close examination of Figures 13 through 16 reveals that a general relationship is apparent between the microwave temperature recorded by the PMIS and the adjusted annual runoff for these watersheds. All four illustrations indicate a trend where larger differences in microwave temperatures are associated with the watersheds producing higher annual runoff. The dashed lines illustrating the general trend in Figures 13, 14, 15, and 16 are estimated. Correlation coefficients (R) were calculated for these plots based on the estimated curves and the annual runoff values. R^2 values were -.272, .501, -.234, and .215, respectively. These values indicate no real relationship is defined by the estimated line in Figures 13 and 15 and the relationship indicated in Figures 14 and 16 is poor.

The scatter of data points in all four plots may indicate that some variables influencing annual watershed runoff are not being sensed with the PMIS. Interflow through the near surface soils is rarely found either in the Rush Spring sandstone or the Chickasha formation, however return flow from groundwater is a major contributor to the annual runoff from most of the eight watersheds. This research has shown that to define groundwater characteristics, microwave sensors would need the capability to penetrate the surface to greater depths than is possible with the present 2.8 centimeter wavelength.

The temporal distribution of rainfall may also be an important consideration in studies of watershed yield as well as the total rainfall. This study did not take into account that the annual rainfall might be a summation of many events producing very little storm runoff or, on the other hand, might be comprised of a few severe storms producing a large part of the annual runoff.

The literature review would indicate that characteristics of watershed surfaces that control groundwater recharge may require the use of more than one wavelength and with one or more long wavelength to penetrate through vegetation and the top soil. There is little evidence in this study to indicate that a usable prediction scheme for annual runoff is possible using the PMIS even though a general relationship is apparent.

The data plotted in Figures 17-20, however, indicate some promising relationships between the PMIS temperatures and storm runoff coefficient. By integrating the numerous parameters influencing the temperature response from a surface, a difference between high or low runoff-producing watersheds can be detected in each of the plots. There are, however, some considerations one should keep in mind before arriving at any conclusions from these plots. First, a significant number of data points (247 to 1,980) from the PMIS were averaged for each watershed and when differences in temperature are considered, twice the number of data points are involved with the single variable ΔT. The coefficient (CN) was developed for each watershed from less than 20 storm events from that watershed. We may therèfore be trying to evaluate the prediction capability of a precise measurement with a crude measurement. This is a common circumstance in testing airborne remote sensors and the reader should keep in mind that the ΔT values are more likely to be statistically

reliable than the coefficient values. The coefficient of variation, the ratio of the standard deviation divided by the mean, was calculated for the microwave temperatures and the storm runoff coefficients (Table 3) to illustrate the relative spread in the data. The values in this table indicate that the coefficient of variation is at least twice as large for the storm runoff values as it is for the microwave temperatures. It would be desirable to have a smaller coefficient of variation for the variable used as ground truth when testing any remote sensing system.

TABLE 3

COEFFICIENTS OF VARIATION

	Watershed Number							
	5141	5142	5143	5144	5146	13	15	25
Mission 227								
σ_v/μ_v	.0119	.0141	.0210	.0150	.0144	.0087	.0069	.0097
σ_h/μ_h	.0238	.0228	.0273	.0261	.0237	.0185	.0136	.0160
Mission 235								
σ_v/μ_v	.0092	.0134	.0121	.0113	.0112	.0248	.0093	.0045
σ_h/μ_h	.0179	.0212	.0203	.0182	.0168	.0451	.0139	.0159
Runoff Coefficient (CN)								
σ/μ	.0370	.0461	.0507	.0390	.0565	.0511	.0468	.0586

Secondly, to a person inexperienced in hydrology, the deviation in the coefficient (CN) from any line through the data points of these plots might appear large. Present manual techniques for calculating such coefficients for watersheds without runoff records are subjective

(Chow, 1964), and sometimes the runoff coefficients are increased to insure that structural design will be on the safe side. The three flood detention structures located below Watersheds 13, 15, and 25 were designed and built for coefficients of 76, 74, and 77, respectively, while measured storms indicate the coefficients should be 46.0, 37.0, and 51.0. The manual method, in this instance, resulted in use of runoff coefficients from 26 to 37 units too large when the structures were designed. Reduction of the overdesign would be significant if the overestimation of the runoff coefficient can be reduced to 10 units or less without permitting the hazards of underdesign.

When selecting a relationship to predict the runoff coefficient, it would be desirable to have the data points fall on a straight line throughout the range of coefficients to provide equal sensitivity for any coefficient. The cross polarized difference in temperature (Fig. 17) shows a lack of sensitivity for runoff coefficients above 55, thus this combination of temperatures from the relatively wet April flight does not appear promising for development of a prediction scheme. For low runoff coefficients, temperature differences are very small, and for the higher coefficients, temperature differences vary 10°K for coefficients above 56.3. This would make the relationship poor in the lower range and unusable in the higher range.

Figure 18, presenting cross polarized differences in temperature for the "dry" late June flight, does appear to more nearly represent a straight line relationship between temperature differences and the runoff coefficient. Temperature differences in this plot for points 25 and 5143 are too large. In Figure 19, where the difference in vertical

polarized temperatures from the wet and dry flights is used, considerable scattering of points is evident. There appears to be no logical explanation for the difference in temperature for Watersheds 25 and 5143 in this plot.

The difference between average horizontal polarized temperature for the two flights would appear to offer the best potential relationship between linear combinations of PMIS temperatures and the runoff coefficient. A best-fit line through the points in Figure 20 would be slightly curved, but could conceivably lead to a prediction scheme for runoff coefficients ranging up to 90. Correlation coefficients were also calculated on the data represented in Figures 17, 18, 19, and 20. The coefficients (R) calculated were .936, .892, .690, and .939, respectively. The R values are based on deviations in runoff coefficients from the estimated curve. The values indicate that the data in Figure 20 is not only sensitive, but is also well correlated.

It was originally proposed that differencing temperature between wet and dry conditions might remove some of the unexplained anomalies seen in microwave temperature. The data presented in these plots would indicate that this thesis was sound, however the data should be examined to determine if any indication is present that separate sets of microwave data from watershed surfaces will produce similar results when related to runoff coefficients. Also, it would be desirable to determine if runoff coefficients can be related to single polarized microwave temperatures collected on a single flight.

A comparison of Figure 17 and Figure 18 shows that a curvelinear relationship exists between the cross polarized differences in temperature and the runoff coefficient. If these plots are superimposed with

the temperature scale matched, it is noticeable that the same general relationship exists for both sets of data, however as the antecedent moisture decreased and vegetation matured, the difference in temperatures, ΔT, decreased and the curve of the data points tends to straighten out. This would lead one to believe that an individual flight, when extremely dry conditions and heavy vegetation prevailed, might produce nearly a straight-line fit to the data. Comparison of these two plots does indicate the repeatability of the relationship.

Again looking at data from individual flights, data for both vertical and horizontal temperatures from each flight can be compared to the runoff coefficients. Figure 21 shows average temperatures for both polarization from each flight plotted individually versus the runoff coefficients. The vertical temperature plots show the slope of the relationship changed direction and the relationship was not good for either flight. The horizontal polarization produces temperatures in both flights that could easily represent a straight-line relation to the runoff coefficient. The late June flight, Mission 235, horizontal temperatures were quite insensitive to changes in runoff coefficients, however the April flight, Mission 227, that was flown over wetter conditions shows a very sensitive relationship between the horizontal polarized temperature and the runoff coefficient. The fact that in both missions the horizontal temperatures and the runoff coefficients can be related by a straight line explains the good linear relation observed when comparing differences in horizontal temperature from the two missions with the runoff coefficients.

It is conceivable that the differences between these two missions shown in Figure 21 can more readily be attributed to differences in

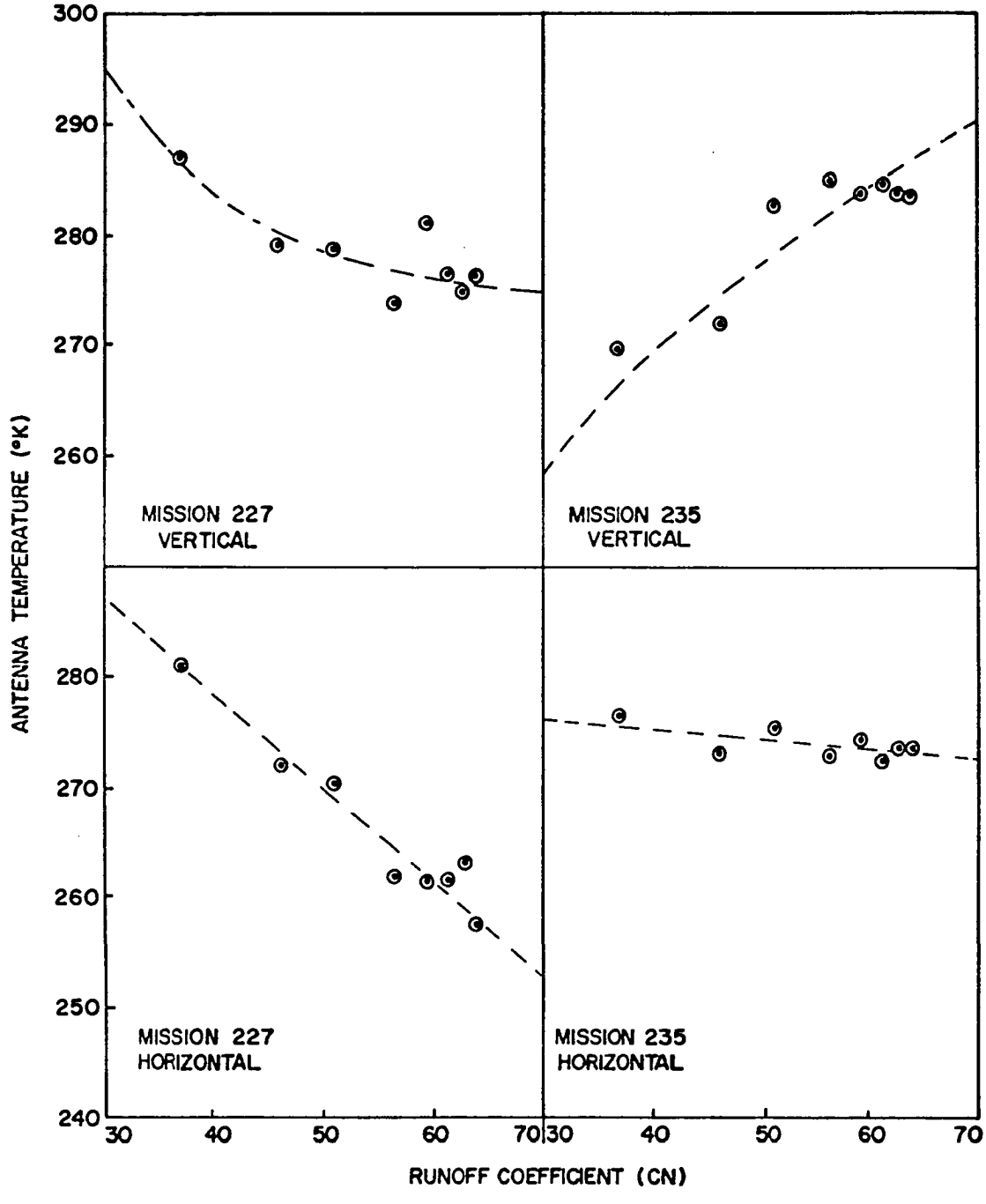

Figure 21. Average Temperatures vs. Runoff Coefficient

vegetation as opposed to differences in moisture conditions. The time period between missions was considerably longer than had been proposed originally and during the period from early or mid-April to late June, major changes in vegetation take place. The antecedent moisture conditions would indicate that lower temperatures would result on both vertical and horizontal polarizations for Mission 235. This did not occur, therefore moisture conditions which should have the predominant effect on temperature apparently had a minor effect on the averages over the watersheds. Roughness sensed with the X-band wavelength of the PMIS should not be greatly different for the two missions. In the literature reviewed, roughness has generally been measured more readily with the horizontal polarization and in these two sets of data we have a linear relation evident in both, while the major change was the change in slope in the plots using vertical polarized temperatures.

If the vegetation was responsible for the difference between the results of the two missions, it would be reasonable to conclude that when depending on a single mission for calibration data, the mission should be scheduled for a dormant period or when vegetation is sparse. Longer wavelength radiometers or multifrequency radiometers with at least one long (20 centimeters or more) wavelength would most likely overcome part of the vegetation problem.

To exploit the relationships indicated in this study, an improvement in the data gathering and processing will be necessary. The microwave data stream to tape on the aircraft should have provision for accompanying surface temperature relative to each beam position along the scan line. This would require a scanning far infrared sensor

synchronized to the microwave imaging system. Data processing from the onboard tape to 9-track tape is presently being reprogrammed by NASA-JSC to incorporate cross polarization corrections that were not in the original processing programs. Some provision should also be made in the new programs to speed up the excerpting of data relevant to any area of the image. Most data extraction programs in the past have removed data from rectangular areas of the image, however, for watershed investigations or geologic studies, irregular shapes are desired. Hopefully, data handling techniques in this study can be used as guidelines for development of systems capable of fast compilation of microwave temperatures pertinent to watershed areas.

Since this experiment involved only eight watersheds, the results can only be viewed as a pilot effort and further testing of the promising relationships should be undertaken.

CHAPTER VII

CONCLUSIONS

1. The difference between horizontal polarized PMIS temperatures from two flights over the same watershed, when vegetation and antecedent moisture conditions were different, were related to the SCS watershed storm runoff coefficient and could reasonably be used to develop a prediction scheme for such coefficients.

2. A sensitive relationship between average PMIS microwave temperatures over a watershed surface and the SCS watershed storm runoff coefficient may be developed using the average horizontal polarization temperatures from a single flight during the dormant or early gorwing season of the year. This relationship could conceivably be used to develop predictions of coefficients.

3. A relationship does exist between differences in the vertical and horizontal polarized average PMIS temperatures over a watershed surface and the SCS storm runoff coefficient however the relationship is unsuitable for prediction of coefficients above 55.

4. Apparent relationships between average PMIS temperatures and average annual watershed runoff do exist however the relationships are poorly defined and indicate that conditions influencing interflow and groundwater contributions are not sensed by the PMIS system.

5. Further testing of this concept of watershed calibration is warranted using the PMIS system and with microwave imagers capable of sensing with longer wavelengths. The testing should extend over a period of 1 year to determine the most appropriate time of year for taking the microwave data.

6. Development of data handling systems capable of more readily extracting the microwave data pertinent to irregular shaped areas will be necessary before practical application of the technique can be made.

BIBLIOGRAPHY

Abdel-Hady, Mohamed, and Karbs, Harlan H. 1971. "Depth to Ground-Water Table by Remote Sensing." Journal of the Irrigation and Drainage Division, Proceedings of the American Society of Civil Engineers, Vol. 97, pp. 355-367.

Alishouse, John C., Baker, Donald R., McClain, E. Paul, and Yates, Harold W. 1972. "Microwave Sensing for Earth Surface Measurements," Instruments and Control Systems, Vol. 45, No. 1, pp. 105-107.

Blanchard, Bruce J. 1972. "Measurements from Aircraft to Characterize Watersheds," 4th Annual Earth Resources Program Review, Vol. V, Agriculture and Forestry Programs, Manned Spacecraft Center, Houston, Texas, pp. 118-1 to 118-14.

Blinn, John C., III, and Quade, Jack G. 1972. Microwave Properties of Geological Materials: Studies of Penetration Depth and Moisture Effects, 4th Annual Earth Resources Program Review, Vol. II, University Programs, Manned Spacecraft Center, Houston, Texas, pp. 53-1 to 53-12.

Bowie, A. J., and Bolton, G. C. 1972. "Variations in Runoff as Influenced by Hydrologic and Physical Characteristics," Proceedings Mississippi Water Resources Conference, Mississippi State University, State College, Mississippi.

Chiang, Sie Ling. 1971. "A Runoff Potential Rating Table for Soils," Journal of Hydrology, Vol. 13, pp. 54-62.

Chow, Ven T., et al. 1964. Handbook of Applied Hydrology, McGraw-Hill Book Company, Inc., New York, Section 21, Hydrology of Agricultural Lands, pp. 21-1 to 21-95 by Ogrosky, H. O., and Mockus, V.

Chow, Ven T. 1962. Hydrologic Determination of Waterway Areas for the Design of Drainage Structures in Small Drainage Basins. University of Illinois Engineering Experiment Station Bulletin No. 462, Urbana, Illinois.

Colcord, J. E. 1972. "Remote Sensing and Photo Interpretation," U. S. Geological Survey, Washington, D. C., Report No. USGS-DO-73-003.

Conway, William, and Yarbrough, Lavern A. 1966. "Characteristics and Uses of an L-Band Radiometer," Proceedings of the Fourth Symposium on Remote Sensing of Environment, Ann Arbor, Michigan, pp. 467-473.

Conway, W. H., Bacinski, R. R., Brugma, F. C., and Falco, C. U. 1963. "A Gradient Microwave Radiometer Flight Test Program," Proceedings of the Second Symposium on Remote Sensing of Environment, Ann Arbor, Michigan, pp. 145-174.

Dutton, John A. 1962. "Space and Time Response of Airborne Radiation Sensors for the Measurement of Ground Variables." Journal of Geophysical Research, Vol. 67, No. 1, pp. 195-205.

Eppler, Walter G., and Merrill, Roy D. 1968. "Correlating Remote Sensor Signals with Ground-Truth Information," Clearing House for Federal Scientific and Technical Information, Springfield, Virginia.

Ewen, H. I., Haneman, F., Kalafus, R. M., Louapre, M. E., Mailloux, R., and Steinbrecher, D. H. 1968. "Microwave Radiometric Capabilities and Techniques." Proceedings of the Fifth Symposium on Remote Sensing of Environment, Ann Arbor, Michigan, pp. 9-58.

Gloersen, P., Wilheit, T., and Schmugge, T. 1972. "Microwave Emission Measurements of Sea Surface Roughness, Soil Moisture, and Sea Ice Structure," 4th Annual Earth Resources Program Review, Vol. 1, Manned Spacecraft Center, Houston, Texas, pp. 8-1 to 8-19.

Hodgin, D. M. 1962. "The Characteristics of Microwave Radiometry in Remote Sensing of Environment," Proceedings of the Second International Symposium on Remote Sensing of Encironment, Ann Arbor, Michigan, pp. 127-137.

Hollinger, James P. 1971. "Remote Passive Microwave Sensing of the Ocean Surface," Proceedings of the Seventh International Symposium on Remote Sensing of Environment, Vol. III, Ann Arbor, Michigan, pp. 1807-1817.

Holtan, H. N. and Lopez, N. C. 1973. "USDAHL-73 Revised Model of Watershed Hydrology," Plant Physiology Institute Report No. 1, Agricultural Research Service, United States Department of Agriculture.

Jean, B. R. 1971. "Selected Applications of Microwave Radiometric Techniques," Technical Report RSC-30, Remote Sensing Center, Texas A&M University, College Station, Texas.

Jean, B. R., Richerson, J. A., and Rouse, J. W., Jr. 1971. "Experimental Microwave Measurements of Controlled Surfaces," Proceedings of the Seventh International Symposium on Remote Sensing of Environment, Vol. III, Ann Arbor, Michigan, pp 1847-1859.

Kennedy, Joseph M. 1971. "Quantitative Values of Soil Moisture from an Airborne Platform," American Geophysical Union, Vol. 52, No. 4,

Kennedy, J. M., and Edgerton, A. T. 1967. "Microwave Radiometric Sensing of Soils and Sediments," Proceedings American Geophysical Union, 48th Annual Meeting.

Kent, K. M. 1973. "A Method for Estimating Volume and Rate of Runoff in Small Watersheds," SCS-TP-149, Soil Conservation Service, U. S. Department of Agriculture.

Kroll, C. L., Sibley, T. G., and Rouse, J. W., Jr. 1973. "Technical Memorandum RSC-69 on the Measuring of Soil Moisture by Microwave Radiometric Techniques," Remote Sensing Center, Texas A&M University, College Station, Texas.

Kunzi, K., Magun, A., Maetzler, C., Schaerer, G., and Schanda, E. 1971. "Passive Microwave Remote Sensing at the University of Bern, Switzerland," Proceedings of the Seventh International Symposium on Remote Sensing of Environment, Vol. III, pp. 1819-1826.

Lee, S. L. 1973. "The Determination of Soil Skin Depth and the Equivalent Soil Moisture Content at Skin Depth," Technical Memorandum RSC-84, Remote Sensing Center, Texas A&M University, College Station, Texas.

Ligon, J. T., and Wilson, T. V. 1971. "Distribution of Moisture in the Unsaturated Profile on a Piedmont Watershed," For presentation at the 1971 Annual Meeting, American Society of Agricultural Engineers.

Linsley, Ray K., Jr., Kohler, Max A., and Paulhus, Joseph L. H. 1949. Applied Hydrology, New York: McGraw-Hill Book Company, Inc.

Louapre, M. E. 1968. "Phased Arrays for Spaceborne Microwave Sensors," Proceedings of the Fifth Symposium on Remote Sensing of Environment, Ann Arbor, Michigan, pp. 59-68.

Lundien, J. R. 1965. "Remote Measurement of Dielectric Constants and Conductivity for Soils," Proceedings of the IEEE, Vol. 53, No. 4, pp. 420-421.

Lundien, J. R. 1971. "Terrain Analysis by Electromagnetic Means," Report No. 5, Technical Report No. 3-693, Laboratory Measurement of Electromagnetic Propagation Constants in the 1.0-1.5 Ghz Microwave Spectral Region, U. S. Army Engineer Waterways Experiment Station, Vicksburg, Mississippi.

MacDowall, J., and Nodwell, B. H. 1971. "Remote Sensing Devices," Report No. 14, Resource Satellites and Remote Airborne Sensing for Canada, Ottawa, Canada.

McAllum, William E. 1973. "Passive Microwave Imaging System Performance Evaluation Flight I," JSC-08656, NASA TM X-58109, Johnson Space Center, Houston, Texas.

Melentyev, V. V. and Rabinovich, Yu. I. 1972. "Emission Properties of Natural Surfaces at Microwave Frequencies," Proceedings of the Eighth International Symposium on Remote Sensing of Environment, Vol. 1, pp. 217-223.

Paris, Jack F. 1969. "Microwave Radiometry and Its Application to Marine Meteorology and Oceanography," Remote Sensing Center, Texas A&M University, College Station, Texas.

Paris, Jack F. 1974. Personal Communication.

Parker, Dana C., and Wolff, Michael F. 1965. "Remote Sensing," International Science and Technology, Vol. 43, pp. 20-31.

Peake, W. H., Riegler, R. L., and Schultz, C. H. 1966. "The Mutual Interpretation of Active and Passive Microwave Sensor Outputs," Proceedings of the Fourth Symposium on Remote Sensing of Environment, Ann Arbor, Michigan, pp. 771-777.

Poe, G., Meeks, D., and Edgerton, A. T. 1971. "Airborne Passive Microwave Measurements of NOAA Hydrology Sites." Report No. 1752FR-1, Aerojet Electro Systems Company, Azusa, California.

Poe, G., Stogryn, A., and Edgerton, A. T. 1971. "Determination of Soil Moisture Content Using Microwave Radiometry," Summary Report 1684R-2, Aerojet-General Corporation, El Monte, California.

Porter, Ronald A. 1969. "An Analytical Study of Measured Radiometric Data," Report No. N 70-20193, Clearing House for Federal Scientific and Technical Information, Springfield, Virginia.

Porter, Ronald A., and Florance, Edwin T. 1969. "Volume III, Feasibility Study of Microwave Radiometric Remote Sensing Additional Plots and Printouts," Report No. 70-14448, Clearing House for Federal Scientific and Technical Information, Springfield, Virginia.

Reynolds, S. G. 1970. "The Gravimetric Method of Soil Moisture Determination, Part I, A Study of Equipment, and Methodological Problems," Journal of Hydrology, Vol. II, pp. 258-273.

Richerson, J. A. 1971. "An Experimental Evaluation of a Theoretical Model of the Microwave Emission of a Natural Surface," Technical Report RSC-27, Remote Sensing Center, Texas A&M University, College Station, Texas.

Riegler, R. L. 1966. "Microwave Radiometric Temperature of Terrain," Contract Report #1903-2, Ohio State University, Columbus, Ohio.

Schmugge, T., Gloersen, P., and Wilheit, T. 1972. "Remote Sensing of Soil Moisture with Microwave Radiometers," Report No. X-652-72-305, Goddard Space Flight Center, Greenbelt, Maryland.

Schmugge, T., Gloersen, P., Wilheit, T., and Geiger, F. 1974. "Remote Sensing of Soil Moisture with Microwave Radiometers," Journal of Geophysical Research, Vol. 79, No. 2, pp. 317-323.

Sers, Sidney W. 1971. "Remote Sensing in Hydrology: A Survey of Applications with Selected Bibliography and Abstracts," Technical Report RSC-22, Remote Sensing Center, Texas A&M University, College Station, Texas.

Sibley, Terrell Gene. 1973. "Microwave Emission and Scattering from Vegetated Terrain." Technical Report RSC-44, Remote Sensing Center, Texas A&M University, College Station, Texas.

Simanton, J. R., Renard, K. G., and Sutter, N. G. 1973. "Procedure for Identifying Parameters Affecting Storm Runoff Volumes in a Semiarid Environment," ARS-W-1, Agricultural Research Service, USDA.

Sinha, Lalit K. 1972. "A Simplified Approach to Predict Surface Runoff and Water Loss Hydrographs," National Symposium on Watersheds in Transition, American Water Resources Association, Urbana, Illinois.

Sowers, George F. 1972. "Remote Sensing for Water Resources," Meeting Preprint No. 1604, American Society of Civil Engineers, National Water Resources Engineering Meeting, Atlanta, Georgia.

Staple, W. J. and Lehane, J. J. 1962. "Variability in Soil Moisture Sampling," Canadian Journal of Soil Science, Vol. 42, pp. 157-164.

Vogel, M. 1972. "Microwave Radiometry at the DFVLR, Oberpfafenhofen, Germany," Proceedings of the Eighth International Symposium on Remote Sensing of Environment, Vol. 1, Ann Arbor, Michigan, pp 199-216.

Waite, W. P., Cook, K. R., Bryan, B. B. 1973. "Broad Spectrum Microwave Systems for Remotely Measuring Soil Moisture Content", Water Resources Research Center Publication No. 18 in cooperation with Engineering Experiment Station Research Report No. 23, University of Arkansas, Fayetteville. 166 pp.

Wiegand, Craig L. 1962. "Drying Patterns of a Sandy Clay Loam in Relation to Optimal Depths of Seeding," Agronomy Journal, Vol. 54, pp. 473-476.

APPENDIX A

WORD LISTING FOR 9-TRACK PMIS TAPE

WORD	CONTENTS	UNITS	DIGITS
1	Time	Hours	Tens
2			Units
3		Minutes	Tens
4			Units
5		Seconds	Tens
6			Units
7	Longitude		Sign
8		Degrees	Hundreds
9			Tens
10			Units
11		Minutes	Tens
12			Units
13			Tenths
14	Latitude		Sign
15		Degrees	Tens
16			Units
17		Minutes	Tens
18			Units
19			Tenths

WORD LISTING FOR 9-TRACK PMIS TAPE--Continued

WORD	CONTENTS	UNITS	DIGITS
20	Radar Altitude	Feet	Ten Thousands
21			Thousands
22			Hundreds
23			Tens
24	Barometric Altitude	Feet	Ten Thousands
25			Thousands
26			Hundreds
27	Heading	Degrees	Hundreds
28			Tens
29			Units
30			Tenths
31	Drift		Sign
32		Degrees	Tens
33			Units
34			Tenths
35	Roll		Sign
36		Degrees	Tens
37			Units
38			Tenths
39	Pitch		Sign
40		Degrees	Tens
41			Units
42			Tenths

WORD LISTING FOR 9-TRACK PMIS TAPE--Continued

WORD	CONTENTS	UNITS	DIGITS
43	Ground Speed	Knots	Hundreds
44			Tens
45			Units
46	Vertical Velocity	10*ft/min	Hundreds
47			Tens
48			Units
49	Time of Year	Years	Tens
50			Units
51		Months	Tens
52			Units
53		Days	Tens
54			Units
55	Mission Identification	Numbers	Hundreds
56			Tens
57			Units
58	Site Number		Hundreds
59			Tens
60			Units
61	Flight Number		Tens
62			Units
63	Line Number		Tens
64			Units
65	Run Number		Tens

WORD LISTING FOR 9-TRACK PMIS TAPE--Continued

WORD	CONTENTS	UNITS	DIGITS
66			Units
67	Radar Mode	Code	
68	System Status 1		
69	System Status 2		
70	System Status 3		
71	System Status 4		
72	System Status 5		
73-116	44 Words Vertical Polarized Signal (V)	Degrees x 10	
117-160	44 Words Horizontally Polarized Signal (H)	Degrees x 10	
161-204	44 Words Up/Down Screen Position (X) (Cross Track)	Degrees x 10	
205-247	44 Words Right/Left Screen Position (Y) (Along Track)	Degrees x 10	
248-292	44 Words Roll in Degrees*10 at Instant of Measurement	Degrees x 10	
293	Scan Number		
294	Sum Used for Vertical Slidelobe Correction		
295-300	Sum Used for Horizontal Slide-lobe Correction		
301	Vertical Raw Baseline		
302	Vertical Raw Calibrate		
303	Horizontal Raw Baseline		
304	Horizontal Raw Calibrate		

WORD LISTING FOR 9-TRACK PMIS TAPE--Continued

WORD	CONTENTS	UNITS	DIGITS
305	Vertical Filtered Baseline		
306	Vertical Filtered Calibrate		
307	Horizontal Filtered Baseline		
308	Horizontal Filtered Calibrate		
309	Antenna Thermistor 1		
310	Antenna Thermistor 2		
311	Average of 4 Antenna Temp.		
312	Radome Thermistor 1		
313	Radome Thermistor 2		
314	Average of 4 Radome Temp.		
315	Bomb Bay Thermistor 1		
316	Bomb Bay Thermistor 2		
317	Average of 4 Bomb Bay Temp.		
318	Horizontal Wave Guide Temp.		
319	Vertical Wave Guide Temp.		
320	Horizontal Hot Load Temp.		
321	Vertical Hot Load Temp.		
322	Horizontal Warm Load Temp.		
323	Vertical Warm Load Temp.		
324	Horizontal Parametric Amp. Temp.		
325	Vertical Parametric Amp. Temp.		
326	Horizontal Enclosure Temp.		
327	Vertical Enclosure Temp.		

WORD LISTING FOR 9-TRACK PMIS TAPE--Continued

WORD	CONTENTS	UNITS	DIGITS
328	Electronic Enclosure Temp.		
329	Pitch	Degrees*10	
330	Drift	Degrees*10	
331	Minutes and Seconds	Binary Total Seconds	
332	Radar Altitude	Feet	
333	Velocity	Feet/Second	

PROGRAM 1

```
001100 IDENTIFICATION DIVISION.                                          PMIS
001200 PROGRAM-ID.  PMIS.                                                PMIS
001300 ENVIRONMENT DIVISION.                                             PMIS
001400 CONFIGURATION SECTION.                                            PMIS
001500   SOURCE-COMPUTER.  IBM-360.                                      PMIS
001600   OBJECT-COMPUTER.  IBM-360.                                      PMIS
001700 INPUT-OUTPUT SECTION.                                             PMIS
001800 FILE-CONTROL.                                                     PMIS
001900     SELECT  FILE-IN  ASSIGN TO   UT-S-FILIN.                      PMIS
002000     SELECT CARD-OUT ASSIGN TO UT-S-FILEOUT.                       PMIS
002100 DATA DIVISION.                                                    PMIS
002200 FILE SECTION.                                                     PMIS
002300 FD  FILE-IN                                                       PMIS
002400     DATA RECORD IS REC-IN                                         PMIS
002500     RECORD CONTAINS 666 CHARACTERS                                PMIS
002600     LABEL RECORDS ARE OMITTED                                     PMIS
002700     RECORDING MODE IS F.                                          PMIS
002800 01  REC-IN.                                                       PMIS
002900     02  TM-HT          PIC S99      COMP.                        PMIS
003000     02  TM-HU          PIC S99      COMP.                        PMIS
003100     02  TM-MT          PIC S99      COMP.                        PMIS
003200     02  TM-MU          PIC S99      COMP.                        PMIS
003300     02  TM-ST          PIC S99      COMP.                        PMIS
003400     02  TM-SU          PIC S99      COMP.                        PMIS
003500     02  FILLER         PIC X(112).                               PMIS
003600     02 LINE-NO         PIC S99      COMP.                        PMIS
003700     02 LINE-NO-TENS    PIC S99      COMP.                        PMIS
003800     02 RUN-NO          PIC S99      COMP.                        PMIS
003900     02 RUN-NO-TENS     PIC S99      COMP.                        PMIS
004000     02 FILLER          PIC X(12).                                PMIS
004100     02  TV    OCCURS 44 TIMES.                                   PMIS
004200         03  V          PIC S99   COMP.                           PMIS
004300     02  TH    OCCURS 44 TIMES.                                   PMIS
004400         03  H          PIC S99   COMP.                           PMIS
004500     02  CX    OCCURS 44 TIMES.                                   PMIS
004600         03  X          PIC S99   COMP.                           PMIS
004700     02  CY    OCCURS 44 TIMES.                                   PMIS
004800         03  Y          PIC S99   COMP.                           PMIS
004900     02  ROLL OCCURS 44 TIMES.                                    PMIS
005000         03  RL         PIC S99   COMP.                           PMIS
005100     02 SCAN-NO         PIC S99      COMP.                        PMIS
005200     02 FILLER          PIC X(80).                                PMIS
005300 FD  CARD-OUT                                                     PMIS
005400     DATA RECORD IS CARDS                                          PMIS
005500     RECORD CONTAINS 80 CHARACTERS                                 PMIS
005600     LABEL RECORDS ARE STANDARD                                    PMIS
005700     BLOCK CONTAINS 0 RECORDS                                      PMIS
005800     RECORDING MODE IS F.                                          PMIS
005900 01  CARDS.                                                        PMIS
006000     02  C-HT           PIC 9.                                    PMIS
006100     02  C-HU           PIC 9.                                    PMIS
006200     02  C-MT           PIC 9.                                    PMIS
006300     02  C-MU           PIC 9.                                    PMIS
006400     02  C-ST           PIC 9.                                    PMIS
006500     02  C-SU           PIC 9.                                    PMIS
006600     02 POINT-1         PIC -----9.                               PMIS
006700     02 VHXY-1          OCCURS 4 TIMES  PIC -----9.               PMIS
006800     02 POINT-2         PIC -----9.                               PMIS
006900     02 VHXY-2          OCCURS 4 TIMES  PIC -----9.               PMIS
007000     02  LINE-1         PIC ----9.                                PMIS
007100     02  RUN-1          PIC ----9.                                PMIS
```

PROGRAM 1--Continued

```
007200      02  SCAN-1       PIC ZZZ9.                                    PMIS
007300  WORKING-STORAGE SECTION.                                           PMIS
007400  77  POINT-CTR    PIC S9(6) VALUE +0 COMP-3.                       PMIS
007500  77  REC-CNT      PICTURE S9(7)  VALUE +0   COMPUTATIONAL-3.       PMIS
007600  77  FC-CNT       PICTURE S9(7)  VALUE +0   COMPUTATIONAL-3.       PMIS
007800  77  X1               PIC S99  VALUE +0  COMP.                     PMIS
007900  77  X2               PIC S99  VALUE +0  COMP.                     PMIS
008000  77  LOW-RNG      PIC S9(3)   VALUE +0    COMP.                    PMIS
008100  77  HI-RNG       PIC S9(3)   VALUE +0    COMP.                    PMIS
008200  77  PRT-CNT      PICTURE Z,ZZZ,ZZ9.                               PMIS
008300  01  WK-AREA.                                                      PMIS
008400      02  FILLER       PIC X(4) VALUE '0000'.                       PMIS
008500      02  NO-UNITS     PIC S9(3) COMP-3 VALUE +0.                   PMIS
008600      02  NO-TENS      PIC S9(3) COMP-3 VALUE +0.                   PMIS
008700  01  WK-MOVE                                                       PMIS
008800  01  CONTROL-CARD                                                  PMIS
008900      02  FILLER       PIC X(14).                                   PMIS
009000      02  SEL-ID       PIC XXX.                                     PMIS
009100      02  FILLER       PIC X(7).                                    PMIS
009200      02  CC-LOW       PIC 9(4).                                    PMIS
009300      02  FILLER       PIC X(6).                                    PMIS
009400      02  CC-HI        PIC 9(4).                                    PMIS
009500  PROCEDURE DIVISION.                                              PMIS
009600  ST.                                                              PMIS
009700      ACCEPT  CONTROL-CARD.                                        PMIS
009800      IF  SEL-ID  =  'ALL'  ALTER RNG-CK TO PROCEED TO GET-DATA    PMIS
009900                    GO TO OPEN-FILES.                              PMIS
010000      IF  SEL-ID  =  'RNG'      GO TO SET-RANGES.                  PMIS
010100  INVALID-CC.                                                      PMIS
010200      DISPLAY 'INVALID CONTROL CARD - '  CONTROL-CARD.             PMIS
010300      GO TO ABEND.                                                 PMIS
010400  SET-RANGES.                                                      PMIS
010500      IF CC-LOW NOT NUMERIC     GO TO INVALID-CC.                  PMIS
010600      IF CC-HI  NOT NUMERIC     GO TO INVALID-CC.                  PMIS
010700      MOVE CC-LOW  TO   LOW-RNG.                                   PMIS
010800      MOVE CC-HI   TO   HI-RNG                                     PMIS
010900  OPEN-FILES                                                       PMIS
011000      DISPLAY CONTROL-CARD.                                        PMIS
011100      OPEN INPUT FILE-IN.                                          PMIS
011200      OPEN OUTPUT CARD-OUT.                                        PMIS
011300  READ-MASTER.                                                     PMIS
011400      READ FILE-IN  AT END  GO TO EOJ.                             PMIS
011500      ADD 1 TO REC-CNT.                                            PMIS
011600  RNG-CK.    GO TO CK-SCAN.                                        PMIS
011700  CK-SCAN.                                                         PMIS
011800      IF SCAN-NO   LOW-RNG      GO TO READ-MASTER.                 PMIS
011900      IF SCAN-NO     HI-RNG     GO TO SCAN-END.                    PMIS
012000  GET-DATA.                                                        PMIS
012100      COMPUTE TM-HT  =  TM-HT - 48.                                PMIS
012200      COMPUTE TM-HU  =  TM-HU - 48.                                PMIS
012300      COMPUTE TM-MT  =  TM-MT - 48.                                PMIS
012400      COMPUTE TM-MU  =  TM-MU - 48.                                PMIS
012500      COMPUTE TM-ST  =  TM-ST - 48.                                PMIS
012600      COMPUTE TM-SU  =  TM-SU - 48.                                PMIS
012700      PERFORM A1 22 TIMES.                                         PMIS
012800      MOVE ZERO TO X1.                                             PMIS
012900      MOVE ZERO TO POINT-CTR.                                      PMIS
013000      GO TO READ-MASTER.                                           PMIS
013100  A1. ADD U TO X1.                                                 PMIS
013200      MOVE TM-HT  TO  C-HT.                                        PMIS
```

PROGRAM 1--Continued

```
013300      MOVE TM-HU  TO  C-HU.                                          PMIS
013400      MOVE TM-MT  TO  C-MT.                                          PMIS
013500      MOVE TM-MU  TO  C-MU.                                          PMIS
013600      MOVE TM-ST  TO  C-ST.                                          PMIS
013700      MOVE TM-SU  TO  C-SU.                                          PMIS
013800      ADD 1 TO POINT-CTR.                                            PMIS
013900      MOVE  POINT-CTR TO POINT-1.                                    PMIS
014000      ADD 1 TO POINT-CTR.                                            PMIS
014100      MOVE  POINT-CTR TO POINT-2.                                    PMIS
014200      COMPUTE VHXY-1 (1)    = V (X1) * 10 / 32.0 + .5.               PMIS
014300      COMPUTE VHXY-1 (2)    = H (X1) * 10 / 32.0 + .5.               PMIS
014400      MOVE X (X1) TO VHXY-1 (3).                                     PMIS
014500      MOVE Y (X1) TO VHXY-1 (4).                                     PMIS
014600      ADD 1 TO X1.                                                   PMIS
014700      COMPUTE VHXY-2 (1)    = V (X1) * 10 / 32.0 + .5.               PMIS
014800      COMPUTE VHXY-2 (2)    = H (X1) * 10 / 32.0 + .5.               PMIS
014900      MOVE X (X1) TO VHXY-2 (3).                                     PMIS
015000      MOVE Y (X1) TO VHXY-2 (4).                                     PMIS
015100      MOVE LINE-NO TO NO-UNITS.                                      PMIS
015200      SUBTRACT 48 FROM NO-UNITS.                                     PMIS
015300      MULTIPLY 10 BY NO-UNITS.                                       PMIS
015400      MOVE LINE-NO-TENS TO NO-TENS.                                  PMIS
015500      SUBTRACT 48 FROM NO-TENS.                                      PMIS
015600      MOVE ZERO TO WK-MOVE.                                          PMIS
015700      ADD NO-UNITS TO WK-MOVE.                                       PMIS
015800      ADD NO-TENS TO WK-MOVE.                                        PMIS
015900      MOVE WK-MOVE TO LINE-1.                                        PMIS
016000      MOVE RUN-NO TO NO-UNITS.                                       PMIS
016100      SUBTRACT 48 FROM NO-UNITS.                                     PMIS
016200      MULTIPLY 10 BY NO-UNITS.                                       PMIS
016300      MOVE RUN-NO-TENS TO NO-TENS.                                   PMIS
016400      SUBTRACT 48 FROM NO-TENS.                                      PMIS
016500      MOVE ZERO TO WK-MOVE.                                          PMIS
016600      ADD NO-UNITS TO WK-MOVE.                                       PMIS
016700      ADD NO-TENS TO WK-MOVE.                                        PMIS
016800      MOVE WK-MOVE TO RUN-1.                                         PMIS
016900      MOVE SCAN-NO TO SCAN-1.                                        PMIS
017000      WRITE CARDS.                                                   PMIS
017100      ADD 1 TO FC-CNT.                                               PMIS
017200 SCAN-END.                                                           PMIS
017300      IF FC-CNT     +0     GO TO EOJ.                                PMIS
017400      DISPLAY 'SCAN NUMBERS LESS THAN HIGH RANGE VALUE'.             PMIS
017500 EOJ.                                                               PMIS
017600      CLOSE FILE-IN.                                                 PMIS
017700      CLOSE CARD-OUT.                                                PMIS
017800      MOVE REC-CNT TO PRT-CNT.                                       PMIS
017900      DISPLAY 'TOTAL RECS READ - '  PRT-CNT.                        PMIS
018000      MOVE FC-CNT TO PRT-CNT.                                        PMIS
018100      DISPLAY 'TOTAL CARDS UNCHED - ' PRT-CNT                        PMIS
018200      COMPUTE REC-CNT  TO  PRT-CNT.                                  PMIS
018300      MOVE RED-CNT  TO  PRT-CNT.                                     PMIS
018400      DISPLAY 'SCAN RECS READ      - '  PRT-CNT.                     PMIS
018500 ABEND.                                                             PMIS
018600      STOP RUN.                                                      PMIS
```

PROGRAM 2

```
// FOR
*ONE WORD INTEGERS
*IOCS(CARD,1132 PRINTER,PLOTTER,TYPEWRITER,KEYBOARD,DISK)
C      IBM 1130 PROGRAM TO AVERAGE POINT NO'S OF EACH LINE OF A MISSION.
       DEFINE FILE 1(3660,16,U,ISEC),2(2450,16,U,ISEC),3(2450,16,U,ISEC)
       DEFINE FILE 4(2850,16,U,ISEC),5(1630,16,U,ISEC),6(2880,16,U,ISEC)
       DEFINE FILE 7(1880,16,U,ISEC),8(1060,16,U,ISEC),9(3280,16,U,ISEC)
       INTEGER X1,Y1,X2,Y2,VV,HH
C      VAVE= AVERAGE VERTICAL TEMP.
C      HAVE= AVERAGE HORIZONTAL TEMP.
C      NOBS= NUMBER OF OBSERVATIONS.
C      MAXV= MAXIMUM VERTICAL TEMP.
C      MINV= MINIMUM VERTICAL TEMP
C      MAXH= MAXIMUM HORIZONAL TEMP.
C      MINH= MINIMUM HORIZONAL TEMP.
C      IP1(I)= FIRST POINT NO. OF RECORD.
C      IV1(I)= FIRST VERTICAL TEMP OF RECORD.
C      IH1(I)= FIRST HORIZONAL TEMP OF RECORD.
C      IP2,IV2,IH2 ARE SECOND POINTS OF RECORD.
C      KTEST= LOWEST VALUE ALOUD.
C      NSL= NUMBER OF SCAN LINES.
       DIMENSION VAVE(44),HAVE(44),NOBS(44)
       DIMENSION MAXV(44),MINV(44),MAXH(44),MINH(44)
       DIMENSION IP1(22),IV1(22),IH1(22),IP2(22),IV2(22),IH2(22)
       WRITE (1,112)
  112  FORMAT (' TURN DATA SWITCH 1 ON FOR PUNCHED OUTPUT')
       WRITE (1,104)
  104  FORMAT (' MISSION 227, FILES NO., 1=L1R1,2=L1R2,3=L2R1,4=L2R2,5=L6
      1R1,6=L6R2,7=L7R1,8=L7R2,9=L8R1')
       WRITE (1,109)
  109  FORMAT ('FILE NO.  KTEST  LINE  RUN')
       WRITE(1,105)
  105  FORMAT ('   XX XXXX   XX    X')
    3  DO 4 I=1,44
       MAXH(I)=0
       MAXV(I)=0
       MINH(I)=9999
       MINV(I)=9999
       NOBS(I)=0
       VAVE(I)=0.0
       HAVE(I)=0.0
       NSL=0
    4  CONTINUE
       ISEC=1
       WRITE (3,110)
  110  FORMAT ('1')
C      INPUT FROM KEYBOARD.
C      IFILE = FILE NUMBER
C      KTEST = LOWEST VALID TEMPATURE.
C      ILINE = LINE NO.
C      IRUN = RUN NO.
       READ (6,103) IFILE,KTEST,ILINE,IRUN
  103  FORMAT (4I5)
    5  DO 65 I=1,22
C      INPUT FROM DISK.
C      RECORDS ARE STORED ON DISK IN HOURS, MINUTES, SECONDS, SCAN POINT NO.,
C      VERTICAL TEMP, HORIZONAL TEMP., X POINT LOCATION, Y POINT LOCATION,
C      SCAN POINT NO., VERTICAL TEMP, HORIZONAL TEMP., X POINT LOCATION,
C      Y POINT LOCATION,  LINE NO., RUN NO., SCAN LINE NO.
```

PROGRAM 2--Continued

```
      READ (IFILE'ISEC)N1,N2,N3,IP1(I),IV1(I),IH1(I),X1,Y1,IP2(I),IV2(I)
     1,IH2(I),X2,Y2,NLINE,NRUN,NSLIN
   65 CONTINUE
      IF (NSLIN) 5,5,99
   99 DO 55 I=1,22
C     TEST FOR TEMPS GREATER THAN 3000.
      IF (IV1(I)-4000) 85,5,5
   85 IF (IV2(I)-3000) 95,5,5
C     TEST FOR TEMPS LESS THAN TEST VALUE.
   95 IF (KTEST-IV1(I)) 75,5,5
   75 IF (KTEST-IV2(I)) 55,5,5
   55 CONTINUE
      NSL=NSL+1
C     TEST FOR MAXIMUM AND MINIMUM OF VERTICAL AND HORIZONAL VALUES.
      II=0
      DO 15 J=1,22

      DO 15 I=1,2
      GO TO (700,701),I
  700 II=II+1
      VV=IV1(J)
      HH=IH1(J)
      GO TO 7
  701 II=II+1
      VV=IV2(J)
      HH=IH2(J)
C     TEST FOR MAXIMUM VERTICAL TEMP.
    7 IF (MAXV(II)-VV)8,9,9
    8 MAXV(II)=VV
C     TEST FOR MINIMUM VERTICAL TEMP
    9 IF (MINV(II)-VV)11,11,10
   10 MINV(II)=VV
C     TEST FOR MAXIMUM HORIZONAL TEMP.
   11 IF (MAXH(II)-HH)12,13,13
   12 MAXH(II)=HH
C     TEST FOR MINIMUM HORIZONAL TEMP.
   13 IF(MINH(II)-HH) 702,702,14
   14 MINH(II)=HH
C     STORES VERTICAL AND HORIZONAL VALUES FOR AVE.
  702 VAVE(II)=VAVE(II)+VV
      HAVE(II)=HAVE(II)+HH
      NOBS(II)=NOBS(II)+1
   15 CONTINUE
C     RETURN TO READ ANOTHER RECORD.
      GO TO 5
   16 DO 17 I=1,44
      VAVE(I)=VAVE(I)/NOBS(I)
      HAVE(I)=HAVE(I)/NOBS(I)
      VAVE(I)=VAVE(I)*.1
      HAVE(I)=HAVE(I)*.1
   17 CONTINUE
      GO TO (781,782),K
  781 WRITE (2,108) NSL
  782 WRITE (3,108) NSL
  108 FORMAT ('    MISSION 219    NO. OF SCAN LINES PROCESSED= ',I5)
      WRITE (3,101)
  101 FORMAT ('    POINT',2X,'MAX.V  MIN.V  MAX.H  MIN.H    AVE.V  AVE.H
     1')
      DO 18 I=1,44
      GO TO (777,778),K
  777 WRITE(2,113)I,MAXV(I),MINV(I),MAXH(I),MINH(I),VAVE(I),HAVE(I),NSL
```

PROGRAM 2--Continued

```
  778 WRITE(3,102)I,MAXV(I),MINV(I),MAXH(I),MINH(I),VAVE(I),HAVE(I)
  102 FORMAT(' ',I4,3X,I5,3(2X,I5),4X,F5.1,2X,F5.1)
  113 FORMAT(' ',I4,3X,I5,3(2X,I5),4X,F5.1,2X,F5.1,25X,I5)
   18 CONTINUE
C     RETURN TO READ ANOTHER DATA SET.
      GO TO 3
   19 CALL EXIT
      END
```

PROGRAM 2A

```
// JOB
// FOR
*LIST ALL
*IOCS CARD,1132 PRINTER
C      IBM 1130 PROGRAM TO AVERAGE VERTICAL AND HORIZONAL TEMPERATURES
C      FOR COMPLETE MISSION
       DIMENSION AVEV(44),AVEH(44)
C      AVEV(I)= TOTAL OF VERTICAL TEMPS.
C      AVEH(I)= TOTAL OF HORIZONAL TEMPS.
C      READ HEADING.
       READ (2,101) A1,A2,A3
       WRITE (3,102) A1,A2,A3
  101  FORMAT (4X,3A4)
  102  FORMAT ('1',3A4)
  105  FORMAT (36X,2F7.1,25X,I5)
       DO 15 I=1,44
       AVEV(I)=0.0
       AVEH(I)=0.0
   15  CONTINUE
       NSA=0
       GO TO 4
C      READ HEADING.
    5  READ (2,101) A1,A2,A3
    4  DO 10 I=1,44
C      AVE=AVERAGE VERTICAL TEMPERATURE FOR POINT.
C      AVH=AVERAGE HORIZONAL TEMPERATURE FOR POINT.
C      NS=NO. OF SCAN LINE IN RUN.
       READ (2,105) AVE,AVH,NS
C      TEST FOR LAST CARD.
       IF (AVE) 6,6,7
    7  AVEV(I)=AVEV(I)+AVE*NS
       AVEH(I)=AVEH(I)+AVH*NS
   10  CONTINUE
C      NSA=TOTAL SCAN LINES IN MISSION.
       NSA=NSA+NS
C      RETURN TO READ ANOTHER DATA SET.
       GO TO 5
    6  DO 20 I=1,44
       AVEV(I)=AVEV(I)/NSA
       AVEH(I)=AVEH(I)/NSA
   20  CONTINUE
       WRITE (3,104) NSA
  104  FORMAT (' ','POINT  AVE.V  AVE.H     NO. OF SCAN LINES=',I5)
       DO 30 I=1,44
       WRITE (3,103) I,AVEV(I),AVEH(I)
  103  FORMAT (' ',I5,2F7.1)
       WRITE (2,900) I,AVEV(I),AVEH(I)
  900  FORMAT (31X,I5,2F7.1)
   30  CONTINUE
   49  CALL EXIT
       END
```

PROGRAM 3

```
// FOR
*IOCS CARD,1132 PRINTER
C      IBM 1130 PROGRAM TO FIND CROSS POLARIZATION FACTORS TO BE USED.
       DIMENSION A(44),B(44),C(44),D(44)
C      A(I)= AVERAGE VERTICAL TEMPS.
C      B(I)= AVERAGE HORIZONAL TEMPS.
C      C(I)= POLARIZATION FACTORS FOR VERTICAL TEMPS.
C      D(I)= POLARIZATION FACTORS FOR HORIZONAL TEMPS.
    2  WRITE (3,105)
  105  FORMAT ('1','CROSS POLARIZATION CORRECTION FACTORS')
C      READS HEADING
       READ (2,106) F1,F2,F3,F4,F5
  106  FORMAT (5A4)
       WRITE (3,107) F1,F2,F3,F4,F5
  107  FORMAT ('0',5A4)
       WRITE (3,104)
  104  FORMAT ('0','POINT      VCORR      HCORR')
       READ (2,101) VMAX,HMIN
C      VMAX= MAXIMUM VERTICAL TEMP.
C      HMIN= MINIMUM HORIZONAL TEMP.
C      VMAX AND HMIN ARE TAKEN FROM PRINTOUT OF AVERAGE VERTICAL AND
C      HORIZONAL PROGRAM.
  101  FORMAT (2F6.1)
       DO 4 I=1,44
    4  READ (2,102) A(I),B(I)
  102  FORMAT (36X,2F7.1)
       DO 5 I=1,44
C      CALCULATES FACTOR FOR POINT OF VERTICAL TEMPERATURE AND STORES IT.
       C(I)=(VMAX-A(I))/(A(I)-B(I))+.00005
C      CALCULATES FACTOR FOR POINT OF HORZIONAL TEMPERATURE AND STORES IT.
    5  D(I)=((B(I)-HMIN)/(B(I)-A(I))+.00005)*(-1.0)
       DO 6 I=1,44
       WRITE (2,103) I,C(I),D(I)
    6  WRITE (3,103) I,C(I),D(I)
  103  FORMAT (' ',I5,3X,F7.4,3X,F7.4)
C      RETURN TO READ ANOTHER DATA SET.
       GO TO 2
   56  CALL EXIT
       END
```

PROGRAM 4

```
// FOR
*ONE WORD INTEGERS
*IOCS(CARD,1132 PRINTER,DISK,PLOTTER)
C      IBM 1130 PROGRAM TO BUILD NEW DATA FILE FROM CROSS POLARIZATION.
       DEFINE FILE 1(3600,16,U,MFILE),2(3600,16,U,IFILE)
       DIMENSION VCORR(44),HCORR(44),N(16)
C      VCORR(I)= VERTICAL TEMP CORRECTION FACTORS.
C      HCORR(I)= HORIZONAL TEMP CORRECTION FACTORS.
C      N(I)= RECORD LENGTH.
       DO 1 I=1,44
     1 READ (2,101) VCORR(I),HCORR(I)
   102 FORMAT (' ',16I6)
   101 FORMAT (6X,2F10.4)
       IFILE=1
       MFILE=1
    20 DO 10 I=1,44,2
     2 READ (1'MFILE) (N(J),J=1,16)
       IF (N(4)) 14,15,14
    14 J1=I
       J2=I+1
C      CALCULATES TEMPERATURE FROM CROSS POLARIZATION FACTORS.
C      CALCULATES FIRST VERTICAL IN RECORD.
       K=(N(5)-N(6))*VCORR(J1)+N(5)
C      CALCULATES SECOND VERTICAL IN RECORD.
       L=(N(10)-N(11))*VCORR(J2)+N(10)
C      CALCULATES FIRST HORIZONAL IN RECORD.
       M=(N(6)-(N(5)-N(6))*HCORR(J1))
C      CALCULATES SECOND HORIZONAL IN RECORD.
       NO=N(11)-(N(10)-N(11))*HCORR(J2)
C      WRITE TO NEW FILE.
       WRITE (2'IFILE) (N(J),J=1,4),K,M,(N(J),J=7,9),L,NO,(N(J),J=12,16)
    10 CONTINUE
C      RETURN TO READ ANOTHER RECORD.
       GO TO 20
C      WRITE LAST RECORD IN FILE.
    15 WRITE (2'IFILE) (N(J),J=1,16)
       CALL EXIT
       END
```

PROGRAM 5

```
// FOR
*ONE WORD INTEGERS
*IOCS(CARD,1132 PRINTER,PLOTTER,TYPEWRITER,KEYBOARD,DISK)
C      IBM 1130 PROGRAM SLICE.
C      ALL FILES AND THIER NO.'S MUST BE ENTERED HERE IF WORKING WITH
C      MORE THAN ONE FILE.
       DEFINE FILE 1(3660,16,U,ISEC),2(2450,16,U,ISEC),3(2450,16,U,ISEC)
       DEFINE FILE 4(2850,16,U,ISEC),5(1630,16,U,ISEC),6(2880,16,U,ISEC)
       DEFINE FILE 7(1880,16,U,ISEC),8(1060,16,U,ISEC),9(3280,16,U,ISEC)
       INTEGER V1,H1,V2,H2,X1,Y1,X2,Y2
       DIMENSION IP(24)
       DATA IP/'A','B','C','D','E','F','G','H','I','J','K','L','M','N','O
      1','P','Q','R','S','T','U','V','W','X'/
C      IP(I)= ARRAY FOR LETTERS.
C      SIZE= LETTER SIZE.
C      THETA= ROTATION OF AXIS.
       SIZE = 1.
       THETA=.01745
C      THIS CARD SHOULD BE CHANGED BEFORE RUNNING ON ANOTHER FLIGHT LINE
C      BECAUSE IT IS PRINTED OUT ON THE TYPEWRITER AND TELLS WHICH FILE
C      NO. TO USE ON WHICH LINE.
    9  FORMAT ('MISSION 219,FILES,1=L1R1,2=L1R2,3=L2R1,4=L2R2,5=L6R1,6=L6
      1R2,7=L7R1,8=L7R2,9=L8R1')
C      SCALE IS IN INCHES PER USERS UNIT.
C      VARIABLE IS ONE FOR VERTICAL AND TWO FOR HORZINTAL TEMPERATURES.
C      NO. SLICES IS HOW MANY LETTERS YOU WISH PLOTTED UP TO TWENTY FOUR.
C      ITEST IS TEMPERATURE WHICH TEMPERATURE'S AT OR BELOW ITEST
C      ARE PLOTTED AS A'S.
C      ALL TEMPERATURES ARE STORED IN THE FILES AS INTERGERS 10 TIMES AS
C      LARGE AS THE REAL TEMPERATURE.
C      INTERVAL IS THE NUMBER OF DEGREES BETWEEN LETTERS X 10,20 WILL
C      GIVE YOU 2 DEGREES BETWEEN LETTERS.
C      LETTER SIZE IS THE SIZE OF THE LETTER TO BE PLOTTED TWO WILL GIVE
C      LETTERS TWO TENTHS HIGH BY TWO TENTHS WIDE.
C      FILE NO. IS THE NO. OF THE FILE TO BE USED IF MORE THAN ONE FILE
C      IS USED OTHERWISE IT IS ONE.
   10  FORMAT('ENTER  SCALE,VARIABLE,NO. SLICES,ITEST,INTERVAL,LETTER SIZ
      1E  FILE NO.')
C      THIS IS PRINTED AFTER FORMAT 10 AND SHOWS WHERE TO ENTER THE DATA
C      AND THE FIELDS ARE RIGHT JUSTIFED.
   11  FORMAT(',XXXXXXXX      X    XX XXXX   XX     X   XX')
       WRITE(1,9)
       WRITE(1,10)
       WRITE (1,11)
C      INPUT FROM KEYBOARD, THESE VARIABLES AGRE WITH FORMAT 10.
    1  READ (6,101)XSCAL,IVAR,NOBS,ITEST,INTV,KSIZE,NFILE
  101  FORMAT(F10.8,6I5)
       ZA = KSIZE/10.
C      TESTS TO SEE IF VARIABLE IS PRESENT
       IF (IVAR)32,32,24
   24  XSCAL = XSCAL*SIZE
       YSCAL = XSCAL
       CALL SCALF(XSCAL,YSCAL,XORG,YORG)
       CALL FPLOT(1,0.0,120.)
       CALL FCHAR(XORG-.2/XSCAL,YORG+120.,ZA,ZA,270.*THETA)
C      WRITES SCALE USED, VARIABLE NO. AND NO. OF SLICES USED. (ON PLOTTER)
       WRITE(7,103)XSCAL,IVAR,NOBS
  103  FORMAT('SCALE = ',F12.8,2X,'VARIABLE = ',I3,2X,'NO. SLICES =',I3)
       CALL FCHAR(XORG-.4/XSCAL,YORG+130.,ZA,ZA,270.*THETA)
```

PROGRAM 5--Continued

```
C     WRITES SMALLEST VALUE TO BE USED FOR AN A TO BE WRITTEN IF TEMP IS
C     LESS THAN ITEST AND WRITES OUT NO OF DEG FOR EACH INTERVAL OF SLICE
      WRITE (7,104)ITEST,INTV
  104 FORMAT('A IS LESS THAN ',I5,2X,'INTERVAL = ',I3,2X,'DEG')
C     JTEST= LARGEST VALUE PLOTTED
      JTEST = ITEST + (NOBS*INTV)
      ISEC=1
   25 READ (NFILE' ISEC)IK,IK,IK,IPT1,V1,H1,X1,Y1,IPT2,V2,H2,X2,Y2,IK,IK
     1,IK
C     TEST FOR END OF FILE
      IF (V1)30,31,30
   30 GO TO (26,27),IVAR
   26 IVAL = V1
C     TEST FOR TOO LARGE A TEMP.
      IF (JTEST-IVAL) 60,29,29
   27 IVAL=H1
C     TEST FOR TOO LARGE A TEMP.
      IF (JTEST-IVAL) 60,29,29
   29 X=X1
      Y = 145.-Y1
      DO 1001 I = 1,NOBS
C     TEST FOR LETTER TO BE AN A.
      IF(ITEST-IVAL)1000,1002,1002
 1000 ITEST = ITEST + INTV
 1001 CONTINUE
 1002 CALL FCHAR(X-.15/XSCAL,Y,ZA,ZA,270.*THETA)
      WRITE(7,102)IP(I)
  102 FORMAT(A1)
C     TEST FOR END OF SCAN LINE.
      IF (I-1) 60,60,55
   55 ITEST=(ITEST-(I-1)*INTV)
   60 GO TO (36,37),IVAR
   36 IVAL = V2
C     TEST FOR TOO LARGE A TEMP.
      IF (JTEST-IVAL)25,49,49
   37 IVAL = H2
C     TEST FOR TOO LARGE A TEMP.
      IF (JTEST-IVAL)25,49,49
   49 X = X2
      Y = 145.-Y2
      DO 2001 J = 1,NOBS
C     TEST FOR LETTER TO BE AN A.
      IF (ITEST-IVAL) 2000,2002,2002
 2000 ITEST = ITEST + INTV
 2001 CONTINUE
 2002 CALL FCHAR(X-.15/XSCAL,Y,ZA,ZA,270.*THETA)
      WRITE (7,102) IP(J)
C     TEST FOR END OF SCAN LINE.
      IF (J-1) 57,57,56
   56 ITEST=(ITEST-(J-1)*INTV)
C     RETURN TO READ 2 MORE DATA POINTS.
   57 GO TO 25
   31 CALL FPLOT(1,(X-.15/XSCAL)+5.0,0.0)
C     RETURN TO BEGIN ANOTHER PLOT.
      GO TO 1
   32 CALL EXIT
      END
```

PROGRAM 6

```
// FOR
*ONE WORD INTEGERS
*IOCS(CARD,1132 PRINTER,DISK)
C       IBM 1130 PROGRAM TO AVERAGE TEMPERATURES WITHIN WATERSHED.
        DEFINE FILE 1(2650,16,U,ISEC)
        DIMENSION IV(44),IH(44)
        DIMENSION N1(22),N2(22),N3(22),IP1(22),IV1(22),IH1(22),N4(22),N5(2
       12),IP2(22),IV2(22),IH2(22),N6(22),N7(22),N8(22),N9(22),ISCAN(22)
C       IV(I)= WORK ARRAY FOR VERTICAL TEMPS.
C       IH(I)= WORK ARRAY FOR HORIZONAL TEMPS.
C       VAVE = AVERAGE VERTICAL TEMP.
C       HAVE= AVERAGE HORIZONAL TEMP.
C       NPT= NUMBER OF POINTS.
        WRITE (3,106)
  106 FORMAT ('1')
C       IMISS = MISSION NUMBER.
C       ILINE = LINE NUMBER.
C       IRUN = RUN NUMBER.
C       IFILE = FILE NUMBER
C       IWATD = WATERSHED NUMBER.
   11 READ (2,104) IMISS,ILINE,IRUN,IFILE,IWATD
  104 FORMAT (5I5)
        ISEC=1
        VAVE=0.0
        HAVE=0.0
        NPT=0
C       READS SCAN LINE, BEGINNG POINT NO., AND ENDING POINT NO. TO BE USED.
    2 READ (2,101) KSCAN,IBEG,ISTOP
  101 FORMAT (11X,3I5)
        J=1
C       TEST FOR END OF FILE.
        IF (KSCAN) 3,60,3
C       SEARCHS FOR RIGHT SCAN LINE.
    3 DO 77 I=1,22
   77 READ(IFILE'ISEC)N1(I),N2(I),N3(I),IP1(I),IV1(I),IH1(I),N4(I),N5(I)
      1,IP2(I),IV2(I),IH2(I),N6(I),N7(I),N8(I),N9(I),ISCAN(I)
C       TEST FOR AGREEMENT OF SCAN LINE NUMBERS.
        IF (ISCAN(1)-KSCAN) 3,4,2
    4 DO 6 I=1,22
        IV(J)=IV1(I)
        IV(J+1)=IV2(I)
        IH(J)=IH1(I)
        IH(J+1)=IH2(I)
        J=J+2
    6 CONTINUE
C       SUMS ALL VALID POINTS.
        DO 7 I=IBEG,ISTOP
        VAVE=VAVE+IV(I)
        HAVE=HAVE+IH(I)
        NPT=NPT+1
    7 CONTINUE
C       RETURN TO READ ANOTHER DATA POINT.
        GO TO 2
C       AVERAGES ALL VALID POINTS IN WATERSHED.
   60 VAVE=VAVE/NPT+.005
        HAVE=HAVE/NPT+.005
        WRITE (3,102) IMISS,ILINE,IRUN,IWATD
  102 FORMAT (' ',' MISSION ',I5,'  LINE ',I5,'  RUN ',I5,'WATERSHED ',I
```

PROGRAM 6--Continued

```
     15)
      WRITE (3,105) VAVE,HAVE,NPT
  105 FORMAT(' ','AVERAGE V = ',F7.1,'  AVERAGE H = ',F7.1,'  NUMBER POI
     1NTS ',I5)
C     RETURN TO READ ANOTHER DATA SET.
      GO TO 11
   70 CALL EXIT
      END
```